UNIVERSITY OF SOUTHERN CALIFORNIA
DEPARTMENT OF CIVIL ENGINEERING

RADIATION DAMPING DURING TWO-DIMENSIONAL IN-PLANE BUILDING-SOIL INTERACTION

by

Maria I. Todorovska and Mihailo D. Trifunac

Report No. CE 91-01

Los Angeles, California
January, 1991

ABSTRACT

The system damping, the system frequency, the relative building response and the base rocking have been studied as those depend on the building mass and height, the flexibility of the soil, the structural damping, the depth of the embedment, the type of incident waves and their angle of incidence. A two-dimensional model has been used which assumes the soil to be a homogeneous isotropic half-space, the foundation supporting the building to be a rigid embedded cylinder and in which the building model is an equivalent single degree-of-freedom oscillator. No coupling has been assumed of the vertical motions with the horizontal motions and the rotation. Both the kinematic and the dynamic interaction effects have been included. Excitations consisting of plane P- and SV-waves have been considered.

TABLE OF CONTENTS

CHAPTER I

INTRODUCTION

Many studies, based on experimental measurements or on theoretical analyses, have shown that the dynamic soil-structure interaction can result in significant modification of the relative response of a structure, of the motion of its footing, and of the motion of the surrounding soil. The flexibility of the foundation medium and the resulting additional degrees of freedom of the building base relative to the incident wave motion make possible a process of radiation of the vibrational energy of the building back into the soil. The final outcome of this process on the relative building response, is reduction of the frequency and of the amplitude of the peak response, relative to the fixed-base model response. An attempt has been made to quantitatively describe the mechanism of the interaction by introducing springs and viscous dampers, attached to the building that would account for the flexibility of the soil and for the, so called, geometric or radiation damping. A pair consisting of a spring and a damper can be defined for each degree of freedom of the foundation. The frequency dependant stiffness and the damping ratios for those springs and dampers can be calculated from the impedance functions for foundations of different shapes (e.g., Apsel and Luco, 1976; Day and Frazier, 1979; Luco and Westmann, 1971), neglecting the coupling terms and using the analogy of a viscously damped single degree of freedom system. Then the building-soil interaction model reduces to a building model connected with springs and dashpots to a rigid base, translating and rotating with the amplitudes of the free-field motion.

The current empirical and analytical methods use such models to estimate the total damping in the building relative response. Methods for representation of the building damping, radiation damping and the damping in the soil, during dynamic building-soil interaction, have been proposed, for example, by Tsai (1974), Rainer (1975), Bielak (1971, 1975, 1976) and Luco (1980). All of those methods use some analogy with a single or a multi degree of freedom (SDOF and MDOF) fixed-base oscillator.

Bielak (1971) and Luco (1980) presented simple analytical expressions for the modal damping ratios, "natural" frequencies and the peak responses for SDOF and MDOF building models on surface foundations, by neglecting the higher order terms of the functions expressing the damping coefficients. In his later work Bielak (1976) arrived at the same analytical expressions assuming orthogonal modes of the flexible-base structure. Bielak (1975) also studied the effect of the depth of the embedment for prismatic three-dimensional foundations. Tsai (1974), assuming orthogonal modes of the flexible-base building, calculated the damping for each mode by matching the shape of the transfer function of his model, with the "actual" transfer function at several locations in the building. Rainer (1975) calculated the total damping for SDOF and MDOF building models (1) measuring the amplitude of the relative building response transfer function at the fundamental system frequency and (2) from the ratio of the energy dissipated during one cycle and the total potential energy during one cycle, associated with a particular mode of vibration. In all those models the kinematic interaction, the coupling terms and the frequency dependant nature of the foundation impedance functions are neglected.

The two-dimensional study of building-soil interaction by Todorovska and Trifunac (1990) showed that the type of incident waves, angle of incidence, and the depth of the embedment may have significant influence on the radiation process. Neglecting the rotation of the incident ground motion and the kinematic interaction may cause nonconservative estimates of the forces in the building. This was seen particularly in the cases for incident Rayleigh waves and for incident plane SV-waves beyond critical angle. In this work this analysis is extended to quantative measurements of the effects of various system factors on the system damping and on the system frequencies. In the work of Todorovska and Trifunac (1990), the building model is a homogeneous shear beam on a rigid circular foundation embedded in a homogeneous and isotopic elastic half-space. It was shown there that the interaction affects significantly only the frequency and the amplitude of the fundamental mode of the building response. In this work the contribution of the higher modes will be neglected. The building will be represented by an equivalent viscously damped single degree of freedom oscillator with rocking degree of freedom relative to the rigid foundation. The response characteristics will be measured directly from the transfer function of the relative building response, including both the dynamic and the kinematic interaction. The system damping will be calculated using the analogy with a damped fixed base single degree of freedom oscillator. The purpose of this study is to see how those are affected by the damping in the building, by the relative building-soil stiffness, by the depth of the embedment and by the type of incident waves and angle of incidence. A two-dimensional model has been chosen first, because it allows analytical closed-form solutions and, thus, better and more explicit understanding of the interaction phenomena.

CHAPTER II

THE MODEL

Ignoring the contribution of the higher modes of vibration to the building response, the building can be represented by an equivalent single degree of freedom (SDOF) oscillator, shown in Fig. II.1, supported by a rigid circular foundation embedded into a homogeneous and perfectly elastic half-space. This oscillator consists of a rod which at one end has a concentrated mass, and at the other end is connected to the foundation at point O through a rotational spring and a rotational dashpot connected in parallel. The mass per unit length in the y- direction of the oscillator is m_b. The center of gravity of this mass is at height H relative to the surface of the foundation, its radius of gyration is r_b, and the vertical connecting "rod" is assumed to be massless. The spring has stiffness constant K_b and represents the rocking stiffness for the oscillator, and the dashpot has damping constant C_b. The width of the foundation is $2a$, the depth of the embedment is h and its mass per unit length is m_f.

The $x-0-z$ coordinate system is an inertial system with origin at the center of the top surface of the foundation at rest. The foundation has three degrees of freedom with respect to this coordinate system: horizontal translation Δ (in the positive x-direction), vertical translation V (in the positive z-direction) and rotation φ (clockwise). The building model has only one degree of freedom with respect to the foundation - the rocking angle ψ^{rel} measured clockwise from the axis ξ, which is always perpendicular to the top surface of the foundation. With respect to the inertial system $x-0-z$, it has horizontal displacement u_b (in the positive x-direction) and vertical displacement v_b (in the positive z-direction). In the linear analysis, there is no coupling between the horizontal and the vertical motions of the mass. Then, the relationships between the displacements of the building and of the foundation are

$$\begin{aligned} u_b &= \Delta + (\varphi + \psi^{\text{rel}})H \\ v_b &= V. \end{aligned} \qquad (II.1)$$

The relative horizontal response $u_b^{\text{rel}} = \psi^{\text{rel}}H$. For a harmonic excitation, with $e^{-i\omega t}$, the system will respond with same frequency, i.e.

$$\begin{aligned} \psi^{\text{rel}} &= \psi_0^{\text{rel}} e^{-i\omega t} \\ \boldsymbol{\Delta} &= \boldsymbol{\Delta}_0 e^{-i\omega t}, \end{aligned}$$

where $\boldsymbol{\Delta} = \{V, \Delta, \varphi H\}^T$ is a generalized displacement vector and $\boldsymbol{\Delta}_0 = \{V_0, \Delta_0, \varphi_0 H\}^T$ is its complex amplitude.

II.1 Motion of the Building

From the free-body diagram (Fig. II.1), neglecting the vertical acceleration $-\ddot{v}_b$, the equilibrium of moments about the center of the base gives

$$m_b \ddot{u}_b H + m_b r_b^2 (\ddot{\varphi} + \ddot{\psi}^{\text{rel}}) + K_b \psi^{\text{rel}} + C_b \dot{\psi}^{\text{rel}} - m_b g (\varphi + \psi^{\text{rel}}) H = 0 \qquad (II.2)$$

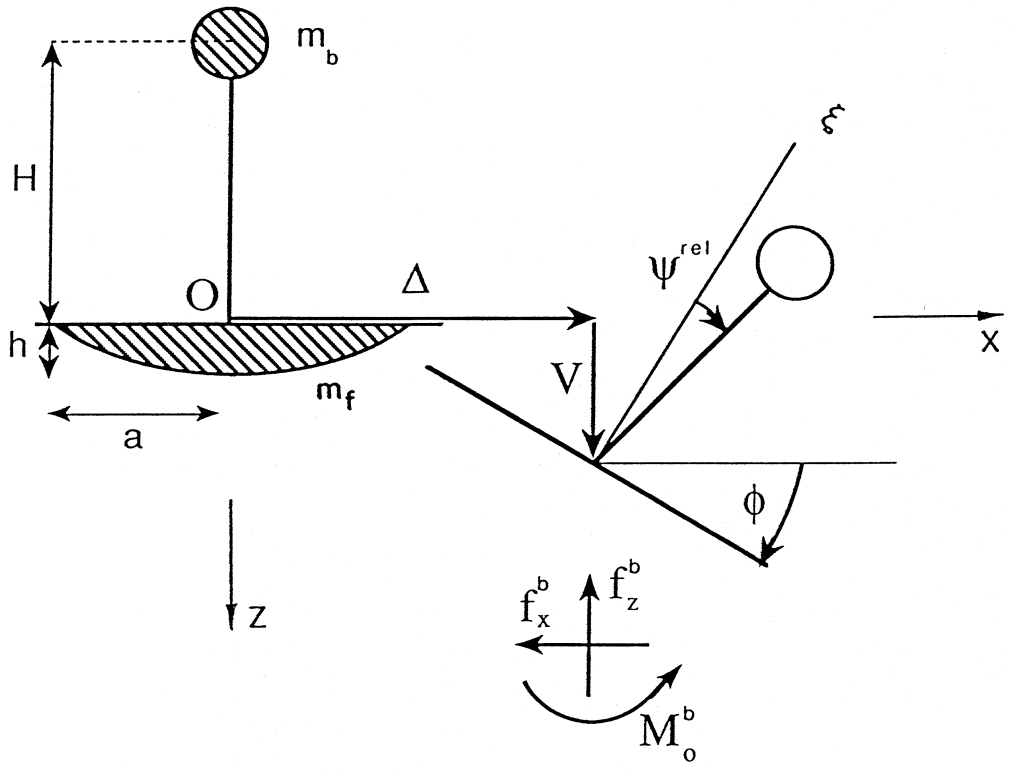

Fig. II.1 The model

where g is the acceleration of gravity. On the left-hand-side of Eq. (II.2), the first term is the moment of the inertia forces due to translation of m_b, the second term is the inertia moment due to rotation of m_b about the point $\xi = 0$, the third and the fourth terms represent the moments of the elastic and of the damping forces and the last term is the moment of the gravity forces.

The equation of motion of the mass m_b, Eq. (II.2), is equivalent to

$$\begin{aligned} &\ddot{\psi}^{\text{rel}} + 2\omega_N \zeta \dot{\psi}^{\text{rel}} + \omega_N^2 \psi^{\text{rel}} \\ &\qquad - \frac{m_b H^2}{I_0} \frac{g}{\omega_N^2 a} \frac{a}{H} \omega_N^2 \psi^{\text{rel}} \\ &\qquad = \frac{-m_b H^2}{I_0} \frac{\ddot{\Delta}}{H} - \ddot{\varphi} + \frac{m_b H^2}{I_0} \frac{g}{\omega_N^2 a} \frac{a}{H} \omega_N^2 \varphi \end{aligned} \tag{II.3}$$

where

$$\frac{K_b}{I_0} = \omega_N^2 \tag{II.4a}$$

$$\frac{C_b}{I_0} = 2\omega_N \zeta. \tag{II.4b}$$

$I_0 = m_b H^2 \left[1 + \left(\frac{r_b}{H}\right)^2\right]$ is the moment of inertia of the building about $\xi = 0$, and ω_N^2 and ζ are the fixed-base natural frequency and the ratio of critical damping. The term $g/\omega_N^2 H$ is a dimensionless parameter involving the acceleration of gravity. For low buildings this ratio is very small ($\sim 10^{-4}$), while for higher buildings it is of order 10^{-1}. For example, for a sixty story building with base $2a = 30$m, it has value ~ 0.3. The damping ratio ζ for typical buildings ranges between 0 and about 0.1. The geometric parameters of the equivalent SDOF building model, H and r_b, are related to the geometric parameters of a shear beam building model, with height H_{sb} and width W_{sb} as

$$H = \frac{H_{sb}}{\sqrt{3}} \tag{II.5a}$$

$$r_b = \frac{W_{sb}}{\sqrt{12}}. \tag{II.5b}$$

For a tall building, for example $H_{sb} = 250$m, $\frac{r_b}{H} \approx 0.08$ and for a short building $\frac{r_b}{H} \approx 0.5$.

For a harmonic motion of the foundation, $\Delta = \Delta_0 e^{-i\omega t}$, from Eq. (II.3), the relative rocking angle ψ^{rel} can be expressed as a function of the displacement of the foundation as

$$\psi_0^{\text{rel}} = \frac{\frac{m_b H^2}{I_0}\left(\frac{\omega}{\omega_N}\right)^2 \frac{\Delta_0}{H} + \left[\left(\frac{\omega}{\omega_N}\right)^2 + \varepsilon_g \frac{m_b H^2}{I_0}\right] \varphi_0}{1 - 2i\zeta\frac{\omega}{\omega_N} - \left(\frac{\omega}{\omega_N}\right)^2 - \varepsilon_g \frac{m_b H^2}{I_0}} \tag{II.6}$$

where $\varepsilon_g = \frac{g}{\omega_N^2 H}$. Then, the forces that the foundation exerts onto the building can be calculated in terms of the displacement of the foundation, from the dynamic equilibrium equations of the structure. Those are

$$\begin{aligned} f_z^{(b)} &= -m_b \ddot{v}_b && (II.7a)\\ &= m_b \omega^2 V_0 e^{-i\omega t} \\ f_x^{(b)} &= -m_b \ddot{u}_b && (II.7b)\\ &= m_b \omega^2 (\Delta_0 + \varphi_0 H + \psi_0^{\mathrm{rel}} H) e^{-i\omega t} \\ M_0^{(b)} &= -m_b \ddot{u}_b H - m_b r_b^2 (\ddot{\varphi} + \ddot{\psi}^{\mathrm{rel}}) + m_b g (\varphi + \psi^{\mathrm{rel}}) H && (II.7c)\\ &= m_b \omega^2 [\Delta_0 H + I_0 (\varphi_0 + \psi_0^{\mathrm{rel}}) + \frac{g}{\omega^2 H} (\varphi_0 + \psi_0^{\mathrm{rel}}) H^2] e^{-i\omega t}. \end{aligned}$$

$f_x^{(b)}$ is positive in the negative x direction, $f_z^{(b)}$ is positive up and $M_0^{(b)}$ is positive counterclockwise. In matrix form one can write

$$\mathbf{F}^{(b)} = m_b \omega^2 \left[[K^{(b)}] + [C_g^{(b)}] \right] \boldsymbol{\Delta}_0 e^{-i\omega t} \qquad (II.8)$$

where

$$\mathbf{F}^{(b)} = \{ f_z^{(b)}, f_x^{(b)}, M_0^{(b)}/H \}^T \qquad (II.9)$$

is a generalized force vector,

$$[K^{(b)}] = \begin{bmatrix} k_{11} & 0 & 0 \\ 0 & k_{22} & k_{23} \\ 0 & k_{32} & k_{33} \end{bmatrix} \qquad (II.10)$$

where

$$k_{11} = 1 \qquad (II.11a)$$

$$k_{22} = 1 + \frac{m_b H^2}{I_0} \left(\frac{\omega}{\omega_N} \right)^2 \frac{1}{p} \qquad (II.11b)$$

$$k_{23} = 1 + \left(\frac{\omega}{\omega_N} \right)^2 \frac{1}{p} \qquad (II.11c)$$

$$k_{32} = k_{23} \qquad (II.11d)$$

$$k_{33} = \frac{I_0}{m_b H^2} \left[1 + \left(\frac{\omega}{\omega_N} \right)^2 \frac{1}{p} \right] \qquad (II.11e)$$

$$p = 1 - 2i\zeta \frac{\omega}{\omega_N} - \left(\frac{\omega}{\omega_N} \right)^2 - \frac{g}{\omega^2 H} \left(\frac{\omega}{\omega_N} \right)^2 \frac{m_b H^2}{I_0} \qquad (II.11f)$$

is the stiffness matrix for the building, and

$$[C_g^{(b)}] = \frac{g}{\omega^2 H} \begin{bmatrix} 0 & 0 & 0 \\ 0 & 0 & c_{23} \\ 0 & c_{23} & c_{33} \end{bmatrix} \qquad (II.12)$$

where

$$c_{23} = \frac{m_b H^2}{I_0} \left(\frac{\omega}{\omega_N}\right)^2 \frac{1}{p} \qquad (II.13a)$$

$$c_{32} = c_{23} \qquad (II.13b)$$

$$c_{33} = 1 + 2\left(\frac{\omega}{\omega_N}\right)^2 \frac{1}{p} + \frac{m_b H^2}{I_0} \left(\frac{\omega}{\omega_N}\right)^2 \frac{1}{p} \frac{g}{\omega^2 H} \qquad (II.13c)$$

is the impedance matrix associated with the gravity forces acting on the building.

II.2 Equilibrium of the Foundation

Fig. II.2 shows the free body diagram of the foundation where $f_x^{(b)}$, $f_z^{(b)}$ and $M_0^{(b)}$ are the horizontal and vertical forces and the moment that the building exerts onto the foundation; $f_x^{(s)}$, $f_x^{(s)}$ and $M_0^{(s)}$ are the horizontal and vertical forces and the moment applied onto the foundation by the elastic half-space; $m_f \ddot{\Delta}$, $m_f \ddot{V}$ and $I_0^{(f)} \ddot{\varphi}$ are the D'Alambert forces of the foundation; and $m_f g$ and point C are its gravity force and center of gravity, respectively. Let $\mathbf{F}^{(s)} = \{f_z^{(s)},\ f_x^{(s)},\ M_0^{(s)}/H\}^T$ and

$$\mathbf{F}^{(s)} = \mathbf{F}_0^{(s)} + \mathbf{F}_\Delta^{(s)} \qquad (II.14)$$

where $\mathbf{F}_0^{(s)}$ and $\mathbf{F}_\Delta^{(s)}$ are generalized force vectors representing the foundation driving forces (forces acting on the foundation at rest and due to the free-field motion) and the forces induced in the half-space due to the deformations caused by the moving foundation, in absence of incident waves. $\mathbf{F}_0^{(s)}$ is equal in magnitude and of opposite direction as the force that must be applied to the foundation to keep it at rest while it is forced to move by the free-field incident waves. Consequently, $\mathbf{F}_0^{(s)}$ depends only on the characteristics of the free-field motion (type of incident waves, angle of incidence and their amplitude), $\mathbf{F}_\Delta^{(s)}$ depends on the imposed motion $\mathbf{\Delta}$, and both depend on the shape of the foundation and on the frequency of excitation. $\mathbf{F}_\Delta^{(s)}$ can be written as

$$\mathbf{F}_\Delta^{(s)} = -2\mu[Q]\mathbf{\Delta} \qquad (II.15)$$

where $2\mu[Q]$ is the impedance matrix for the foundation and μ is the shear modulus of the half-space. The expressions for $\mathbf{F}_0^{(s)}$, for incident plane P- and SV- and surface Rayleigh waves, as well as for $[Q]$ can be found in Todorovska and Trifunac (1990).

The equilibrium equations of the foundation are

$$[M_f]\ddot{\mathbf{\Delta}} = \mathbf{F}^{(b)} - \mathbf{F}^{(s)} - \mathbf{F}_g^{(f)} \qquad (II.16)$$

where

$$[M_f] = \mathrm{diag}\{m_f,\ m_f,\ I_0^{(f)}/H^2\} \qquad (II.17)$$

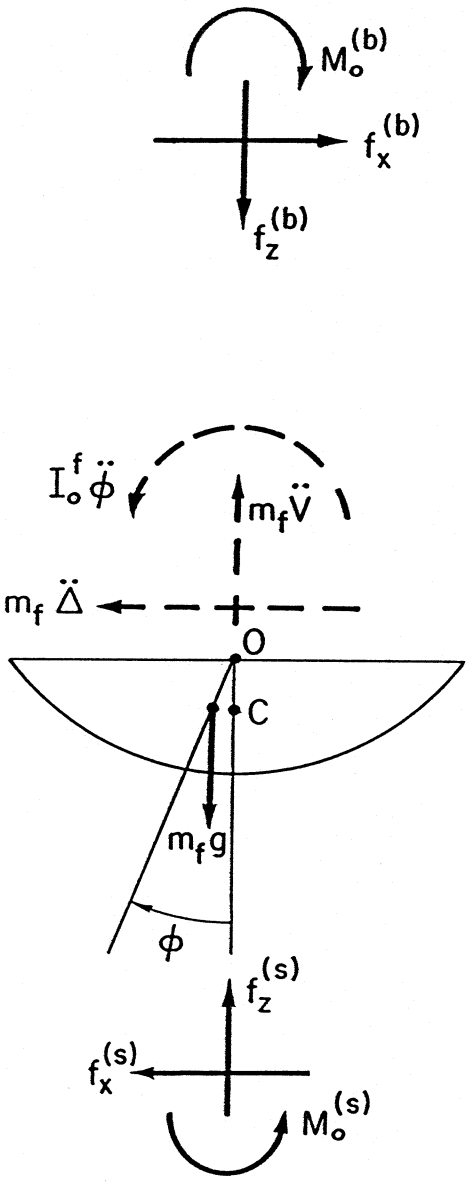

Fig. II.2 Equilibrium of forces acting on the foundation

is the mass matrix of the foundation ($I_0^{(f)}$ is its moment of inertia about point O) and

$$\mathbf{F}_g^{(f)} = \{0, 0, \; m_f g \frac{c}{H} \varphi\}^T \qquad (II.18)$$

is the generalized force vector of the gravity forces of the foundation (c is the depth to the center of gravity). Then for given characteristics of the structure and for various types of excitation, Eq. (II.16) can be solved for $\mathbf{\Delta}$.

CHAPTER III

RESULTS AND ANALYSIS

III.1 System Parameters

Definition of the Dimensionless Parameters

Since the intensity of scattering of the waves from the building foundation and the interaction between the building motion and the soil depend on the size of the foundation relative to the wavelength of the incident waves, and on the stiffness of the building, compared with the stiffness of the soil, the dimensionless quantities $\eta = \frac{2a}{\beta T} = \frac{\omega a}{\pi \beta}$ and $\eta_N = \frac{2a}{\beta T_N} = \frac{\omega_N a}{\pi \beta}$, respectively, will be used in the analysis, rather than the frequencies ω and ω_N. The meaning of η is the number of wavelengths of the S waves in the soil, with frequency ω, contained in length equal to the width of the foundation. Then η_N is the value of η when the frequency of the S waves is equal to the natural frequency of the building, ω_N. Other dimensionless parameters that affect the response of the building-foundation-soil system are the mass ratios $\frac{m_b}{m_f}$ and $\frac{m_f}{m_s}$, where m_s is the mass of the soil replaced by the foundation. Typically, the ratio of the mass density of the building and of the soil is $\frac{\rho_b}{\rho_s} = 0.2$. We assume in our calculations that the foundation and the building have the same mass density ($\rho_b/\rho_f = 1$). Accordingly, $\frac{m_f}{m_s} = 0.2$ and $\frac{m_b}{m_f} \approx 2.2\frac{H}{a}$ for a semi circular foundation $\left(\frac{h}{a} = 1\right)$ and $\frac{m_b}{m_f} \approx 4.9\frac{H}{a}$ for a foundation with depth to-half-width ratio $h/a = 0.5$, for example. Typically η_N ranges in the interval 0 - 0.6 and H/a between 0.5 - 3 (Luco, 1980). We considered in this analysis the building damping ratio $0 \leq \varsigma \leq 0.12$.

For example, for a 10 story building (natural frequency $f_N = 1$Hz and base half-width $a = 15$m), situated on medium soft soil with shear wave velocity $\beta = 400$m/s, for the lumped mass model $H/a \approx 1.9$ and $\eta_N \approx 0.076$. On the other hand, for a nuclear power plant containment structure (natural frequency $f_N = 5H_z$ and $a = 23$m) situated on harder soil ($\beta = 800$ m/s) $\eta_N \approx 0.28$. The same 10 story building in Los Angeles ($\beta \approx 250$m/s) would have $\eta_N \approx 0.15$, and in Mexico City, where the shear wave velocity in the soil can be as low as $\beta = 50$ m/s, $\eta_N \approx 0.3$.

Selection of the System Parameters

We consider incident plane SV-waves, with indent angles $\gamma = 0°$, $20°$, $30°(= \gamma_{\text{crit}})$ $45°$, $60°$ and $85°$, where γ_{crit} is the critical angle, and incident plane P-waves (Todorovska and Trifunac, 1990), with indent angles $\gamma = 0°$, $30°$, $60°$ and $85°$. The Poisson's ratio $\nu = 0.3333$. The effect of the gravity forces is neglected.

To see the effect of the depth of the embedment, we varied the depth-to-half-width ratio of the foundation h/a in the interval $h/a \in [0.5, 1]$. We encountered difficulties in the numerical calculations if h/a was much smaller than 0.5. Calculating the Bessel functions

of very high order and small argument with sufficient accuracy (smaller values of h/a require more terms in the series than for $h/a = 1$) is difficult. However no significant advantages for this analysis were expected for foundation shallower than $h/a = 0.5$, that would warrant the effort required to improve the accuracy of the numerical computations.

We varied η_N in the interval (0,0.3]. However in many of the cases considered, it was not possible to calculate the equivalent damping ratio since the peak of the relative response was too low and wide. We will present most results with maximum value of $\eta_N = 0.2$.

We calculated the response for low, medium, high and very high buildings (compared with the size of their base), for $H/a = 0.5$, 2, 5 and 10. In all the cases the density of the foundation is one fifth of the density of the half-space ($\frac{m_f}{m_s} = 0.2$). Then, for each value of H/a, we calculated the value of $\frac{m_b}{m_f}$ that corresponds to $\rho_b/\rho_s \approx 0.2$. For a semi-circular foundation $\frac{m_b}{m_f} = 2\frac{H}{a}$ and for shallow foundations with $h/a = 0.5$ $\frac{m_b}{m_f} = 4\frac{H}{a}$. Furthermore, we considered values for $\frac{m_b}{m_f}$ twice larger and twice smaller than the value that corresponds to $\rho_b/\rho_s = \rho_b/\rho_f \approx 0.2$, to see how the value of m_b/m_f affects the damping ratio when H/a and $\frac{m_f}{m_s}$ are kept constant. The structural damping ratio we varied in the interval $\varsigma \in (0, 0.12]$.

In our analysis we also considered extreme cases, such as very tall and very "heavy" buildings and high structural damping, because understanding those can help understand the trends of the "intermediate" cases. In this study, understanding the system behavior in the case of very "strong" interaction effects helped us explain its behavior for "moderate" interaction effects.

Definition of System Frequency and System Damping

In previous studies (e.g., Bielak, 1971; Luco, 1980; and Todorovska and Trifunac, 1990), it was shown that the soil-structure interaction modifies the amplitudes and the shape of the transfer function between the building relative response and the incident wave motion. It was shown that the interaction changes the amplitudes and the frequencies of the peaks of the transfer function, relative to the fixed-base model transfer function. In the vicinity of the peak frequencies the base rotation is large. The frequencies are changed because of the flexibility of the foundation medium, and the peak responses are changed because of the radiation of the building vibrational energy into the soil. The transfer function of a flexible-base building model resembles the transfer function of a fixed-base building model. By "system frequency" and by "system damping ratio" we will refer to the frequency and to the usual measure of the width of the peak of the amplitude of the flexible-base model transfer function. The system frequency will be expressed in terms of the dimensionless frequency η and will be denoted by η^{sys}, while the system damping ratio will be denoted by ς^{sys}.

We will measure the equivalent damping ratio, ς^{sys}, from the amplitude spectrum of the transfer function between the relative building response, $u_b^{rel} = \psi^{rel} H$ and the incident wave motion, using the analogy with the half-power method for a SDOF oscillator. Thus we will measure the frequency of the peak of the response, η^{sys}, and the frequencies to the left and to the right of η^{sys} (η_1 and η_2) for which $u_b^{rel} = u_b^{rel}(\eta^{sys})/\sqrt{2}$. Then ς^{sys} can be calculated as

$$\varsigma^{sys} = \frac{\eta_2 - \eta_1}{\eta_1 + \eta_2} \approx \frac{\eta_2 - \eta_1}{2\eta^{sys}}. \qquad (III.1)$$

The relative building response was calculated using to the equations in the previous section, and solving the system of equations (II.16) for $\mathbf{\Delta}$. No additional approximations and assumptions, were made. To reduce the calculation effort, the foundation driving force $\mathbf{F}_0^{(s)}(\eta)$ and the matrix $[Q(\eta)]$ were calculated only once (at selected frequencies) for a given type of excitation and foundation shape. Their values were then substituted in Eq. (II.16) for different combinations of the remaining parameters. The damping was measured from the transfer function amplitude, calculated from Eq. (II.16) at frequencies equally spaced at $\Delta\eta = 0.0017125$. Cubic spline interpolation was used in the numerical search for the peak response and for the frequencies η_1 and η_2 in Eq. (III.1).

III.2 Vertically Incident SV-waves and Semi-Circular Foundation

For vertically incident SV-waves, the free-field motion, u^{ff}, (motion resulting from the interference of the incident wave and the wave reflected from the half-space surface in absence of any inhomogeneities or irregularities) does not have a rotational component or a vertical component, on the ground surface. However, due to the embedment, the foundation input motion (response of a massless foundation in the absence of the superstructure) does experience a rotation (Todorovska and Trifunac, 1990) because of the finite size of the embedment, relative to the wavelength of the incident waves, and because of the anti-symmetric nature of the displacement of the free-field motion, with respect to the vertical axis of symmetry of the foundation. So, in general the foundation will rotate because of the rotation of the foundation input motion and because of the action of the forces exerted by the superstructure.

The dimensionless parameter η_N depends on the ratio of the stiffness of the building and of the half-space and on the ratio of the mass of the building and the mass of the soil replaced by the foundation. For a semi-circular foundation

$$\eta_N = \frac{\omega_N a}{\pi\beta} = \sqrt{\frac{K_b}{\mu a}}\sqrt{\frac{m_s}{m_b}}\sqrt{\frac{2}{\pi^3}} \cdot \frac{1}{\sqrt{1 + \left(\frac{r_b}{H}\right)^2}} \frac{a}{H}. \qquad (III.2)$$

Small η_N means a flexible building and/or stiff soil and large η_N means a stiff building and/or very flexible soil. The limiting value $\eta_N \to 0$ corresponds to the case of a flexible building on a rigid half-space excited by horizontal motion at the base $\Delta = 2e^{-i\omega t}$ (fixed-base buildings model, no interaction). $\eta_N \to \infty$ corresponds to a rigid building oscillating

together with the foundation as a single rigid body, with translational and rocking degrees of freedom.

In Fig. III.2.1, the system damping, ς^{sys}, the system frequency, η^{sys}, the amplitude of the peak relative building response, $|u_b^{rel}(\eta^{sys})|$, and the amplitude of the peak base rotation, $|\varphi(\eta^{sys})a|$, have been plotted versus the "relative stiffness" parameter η_N for a typical building ($H/a = 2$), with damping ratios $\varsigma = 0.005$, 0.05 and 0.12, and mass ratios $m_b/m_f = 2$, 4 and 8. In Fig. III.2.2, the same quantities are shown as functions of ς, for a building with same values of H/a and m_b/m_f, and for $\eta_N = 0.05$ and 0.2. In Fig. III.2.3 and Fig. III.2.4 the same functional relationships are shown as in Fig. III.2.1 and Fig. III.2.2, but for a higher building ($H/a = 5$ and m_b/m_f =5, 10 and 20). Since the system frequency does not depend on the damping in the building, in Fig. III.2.1 and Fig. III.2.3 η^{sys} versus η_N is shown only for $\varsigma = 0.05$.

Asymptotic Behavior as $\eta_N \to 0$ and as $\eta_N \to \infty$

When the soil is stirrer, the system response is influenced more by the damping in the building, while when it is more flexible it is affected more by the building mass and height. This can be concluded from Fig. III.2.1 and Fig. III.2.3, where as $\eta_N \to 0$ the curves corresponding to same value of ς merge together, while as $\eta_N \to \infty$ the curves with same value of m_b/m_f merge together.

As $\eta_N \to 0$ the relative building response u_b^{rel} has similar features as for the fixed-base building response ($\eta^{sys} \to \eta_N$, $\varsigma^{sys} \to \varsigma$, $u_b^{rel}(\eta^{sys}) \to u_b^{rel}(\eta_N)$ and $\varphi \to 0$). Then the dissipation of the vibrational energy through radiation into the soil is very small. As $\eta_N \to \infty$, $\varsigma^{sys}(\eta_N)$, $\eta^{sys}(\eta_N)$ and $\varphi(\eta_N)$ have horizontal asymptotes that depend on the building mass and height and $u_b^{rel}(\eta^{sys}) \to 0$. Then $\eta^{sys} \to \eta^{rig}$, the system frequency of the building-foundation rigid body motion which is lower when the building is "heavier." The rocking of the base $\varphi \to \varphi^{rig}$, the base rocking when the building is rigid, which is larger when the building mass is larger (Todorovska and Trifunac, 1990). (The foundation mass in all the examples is small compared with the building mass and does not play a major role.) The value of ς^{sys} then only reflects the shape of the peak of the spectra $|u_b^{rel}(\eta)|$, which is similar with the shape of the peak of the spectra $|\varphi(\eta)|$. The peak of $|\varphi(\eta)|$ is sharper and higher when the building is higher and heavier and, therefore, the system damping ratio is smaller when the building mass is larger and when the building is higher.

System Behavior for Intermediate η_N

When the soil is flexible, for given shape of the foundation and for given building height, the peak relative building response is smaller, the peak base rocking response is larger and the system frequency is lower when the building mass is larger (Fig. III.2.1 and Fig. III.2.3). When the soil is stirrer (lower η_N), the system damping ratio is larger for

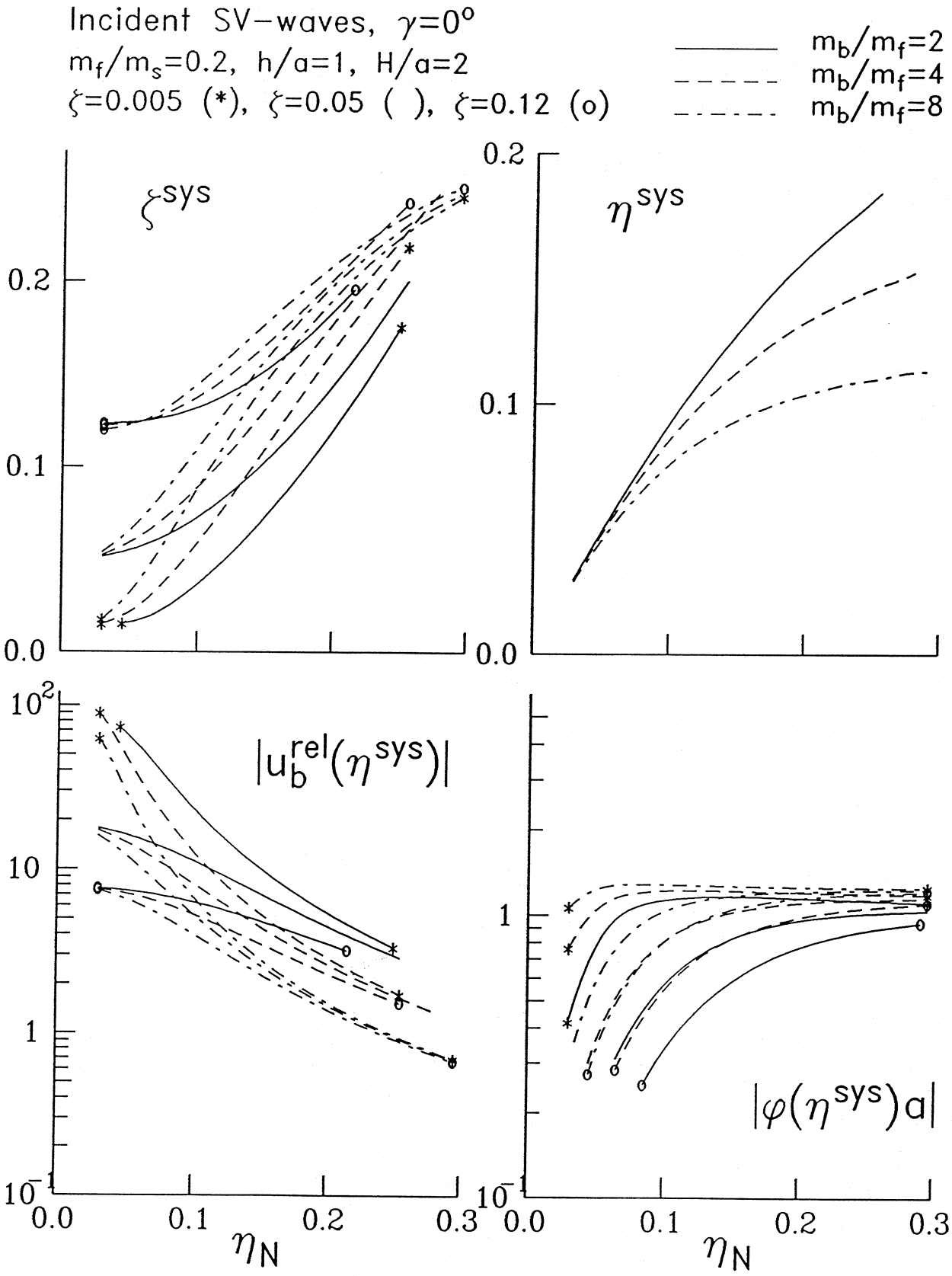

Fig. III.2.1 The system damping ζ^{sys} ratio, the system frequency η^{sys}, the peak relative building response $u_b^{rel}(\eta^{sys})$ and the peak base rocking response $\varphi^{rel}(\eta^{sys})a$ versus the relative stiffness parameter, η_N, for a medium high building $(H/a = 2)$ on a semi-circular foundation.

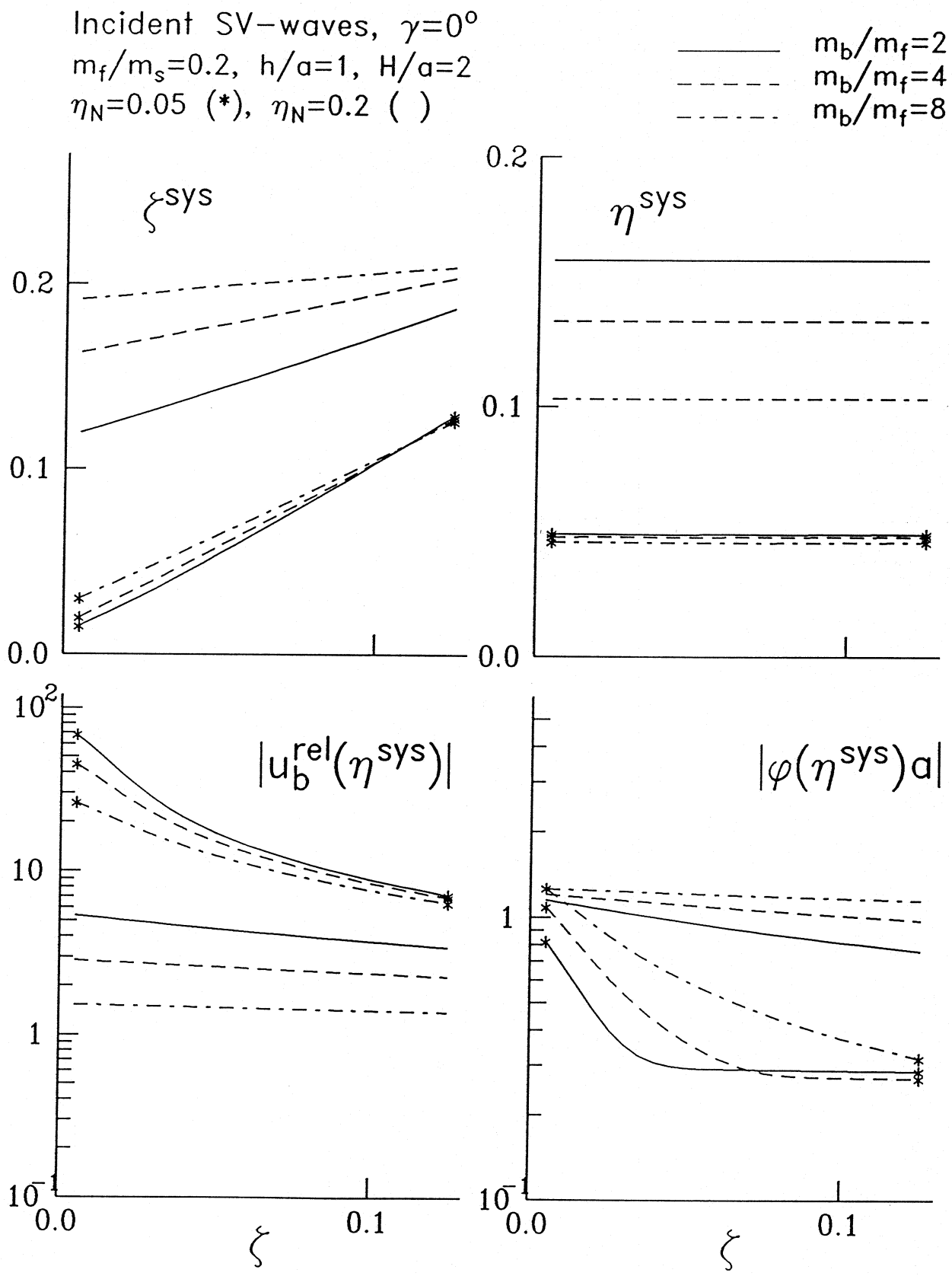

Fig. III.2.2 The system damping ζ^{sys} ratio, the system frequency η^{sys}, the peak relative building response $u_b^{rel}(\eta^{sys})$ and the peak base rocking response $\varphi^{rel}(\eta^{sys})a$ versus the damping ratio in the building, ζ, for a medium high building $(H/a = 2)$ on a semi-circular foundation.

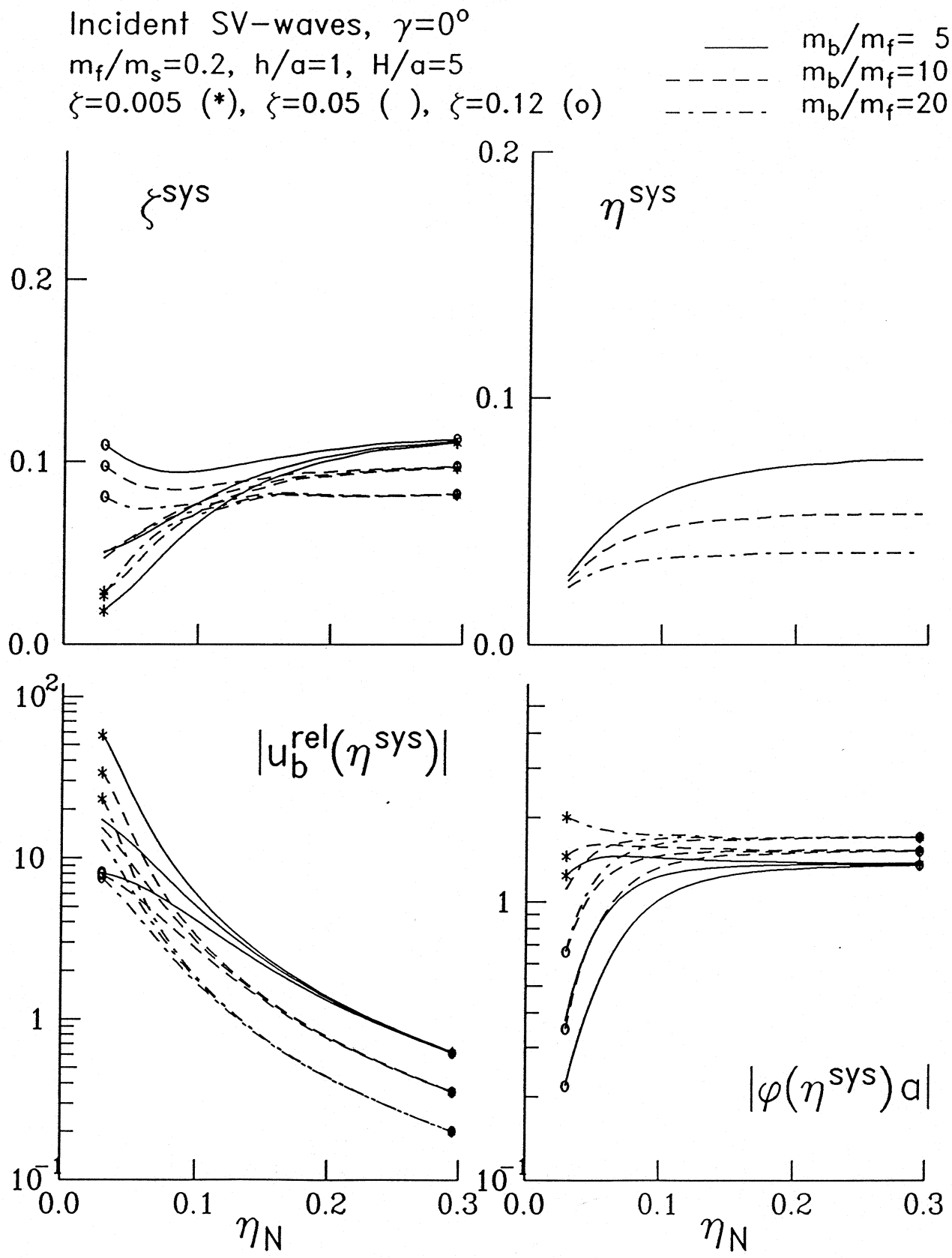

Fig. III.2.3 The system damping ζ^{sys} ratio, the system frequency η^{sys}, the peak relative building response $u_b^{rel}(\eta^{sys})$ and the peak base rocking response $\varphi^{rel}(\eta^{sys})a$ versus the relative stiffness parameter, η_N, for a higher building $(H/a=5)$ on a semi-circular foundation.

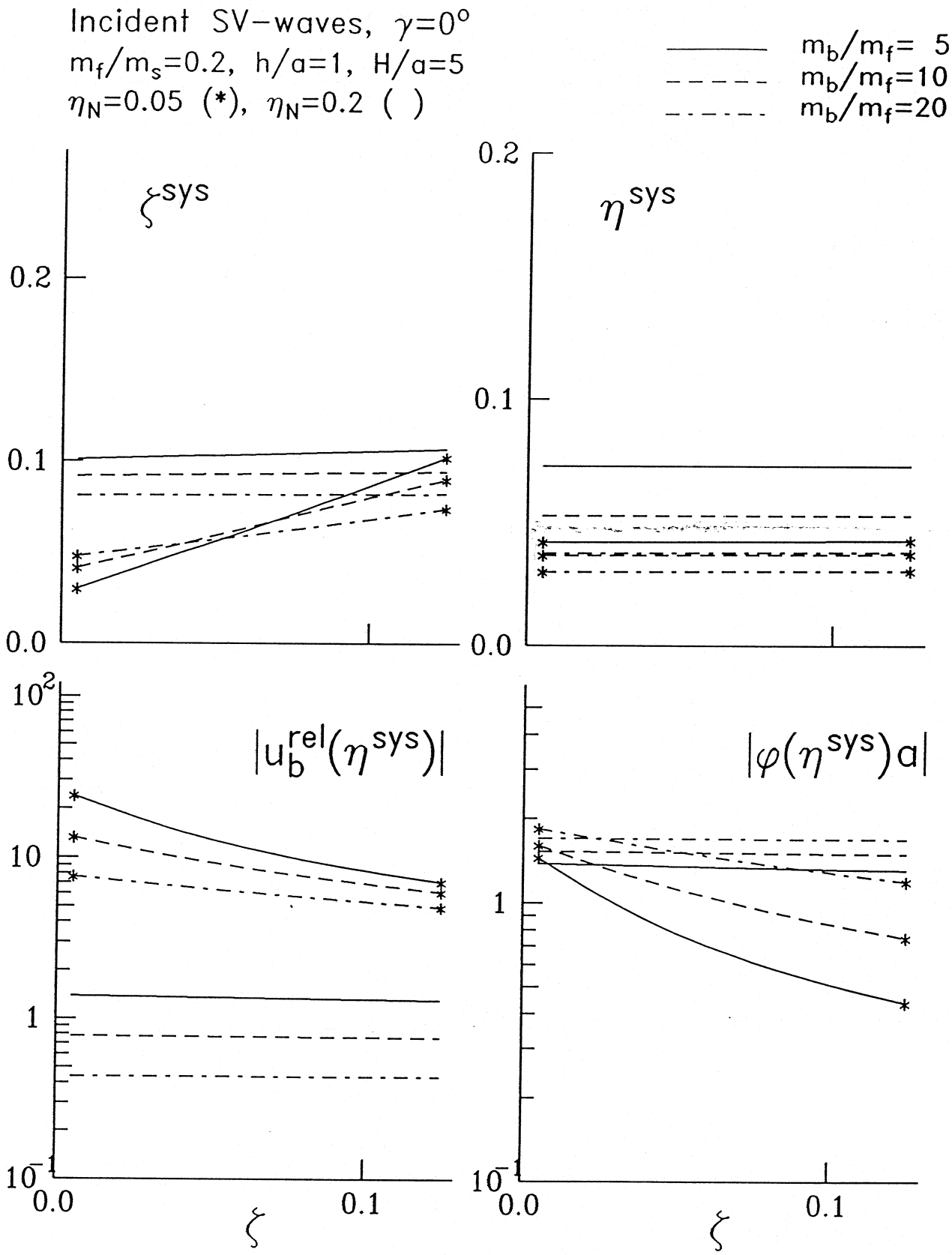

Fig. III.2.4 The system damping ratio ζ^{sys}, the system frequency η^{sys}, the peak relative building response $u_b^{rel}(\eta^{sys})$ and the peak base rocking response $\varphi^{rel}(\eta^{sys})a$ versus the damping ratio in the building, ζ, for a higher building $(H/a=5)$ on a semi-circular foundation.

"heavier" buildings. However, for sufficiently large η_N, when the building behaves more like a rigid body, it is smaller when the building is "heavier."

The relative building response $u_b^{\text{rel}}(\eta^{\text{sys}})$ always decreases as the flexibility of the soil increases. However, the system damping ratio may increase or decrease, depending on how large the damping ratio in the building is compared with ς^{rig}, the asymptotic value of the system damping ratio as $\eta_N \to \infty$. In most of the cases that we considered $\varsigma < \varsigma^{\text{rig}}$ and ς^{sys} monotonically increases with increasing η_N. However, in the extreme case of vary high structural damping ($\varsigma = 0.12$) and a high building ($H/a = 5$), $\varsigma > \varsigma^{\text{rig}}$. Then, as η_N increases and the contribution of the building damping ratio to ς^{sys} becomes smaller, the system damping decreases. Then, as the example shows, $\varsigma^{\text{sys}} < \varsigma$ does not mean that the relative building response is larger than the response on "rigid" soil.

It can be seen from Fig. III.2.1 and III.2.3 that, in the lower range of η_N, the base rocking, $|\varphi(\eta^{\text{sys}})|$, is larger when the soil is more flexible. It is larger when the building damping is smaller. For sufficiently high η_N, when the building behaves more like a rigid body, as η_N increases, $|\varphi(\eta^{\text{sys}})|$ approaches monotonically the limit, which is the rocking response of a rigid building. It may monotonically increase or decrease while approaching this limit depending on how large it had grown in the region of lower values of η_N.

System Response versus ς

From the curves in Fig. III.2.2 and Fig. III.2.4, the following can be seen. The system frequency η^{sys} does not depend on ς. The relative building response decreases with zeta at a higher rate when the building is lower, lighter and on harder soil and it practically does not depend on ς when the building is higher, heavier and on sufficiently soft soil.

All the curves $\varsigma^{\text{sys}}(\varsigma)$ are practically straight lines with slope having values between 1 and 0 and value at $\varsigma = 0$ depending on m_b/m_f, H/a and η_N. Because there is no damping in the soil, when $\varsigma = 0$ the system damping is due only to radiation and scattering. For the lower and lighter building ($H/a = 2$ and $m_b/m_f = 1$, Fig. III.2.2), when the building is sitting on harder soil ($\eta_N = 0.05$), the slope is close to 1 and $\varsigma^{\text{sys}}(0)$ is small. For the lower and lighter building ($H/a = 2$ and $m_b/m_f = 1$, Fig. III.2.2, when the building is sitting on harder soil ($\eta_N = 0.05$), the slope of $\varsigma^{\text{sys}}(\varsigma)$ is close to 1 and $\varsigma^{\text{sys}}(\varsigma = 0)$ is small. For heavier buildings (Fig. III.2.2) and on softer soil ($\eta_N = 0.2$), the slope of $\varsigma^{\text{sys}}(\varsigma)$ is small (the rate of change of ς^{sys} with ς is small) and $\varsigma^{\text{sys}}(\varsigma = 0)$ is larger. ς^{sys} practically does not depend on ς when $H/a = 5$ and $m_b/m_f = 5$, 10 and 20 (Fig. III.2.4). It can be concluded that, for a tall and heavy building, the system damping practically does not depend on the damping in the building.

When the building is lower and when it is on harder soil ($H/a = 2$, $\eta_N = 0.005$), system damping ratio is larger when the building mass is larger. For the higher building and on softer soil ($H/a = 5$ and $\eta_N = 0.2$, Fig. III.2.4), on the contrary, for all values of ς the system damping ratio is smaller when the building mass is larger (the system behaves "more like a rigid body"). From the values of ς at which the curves for different values

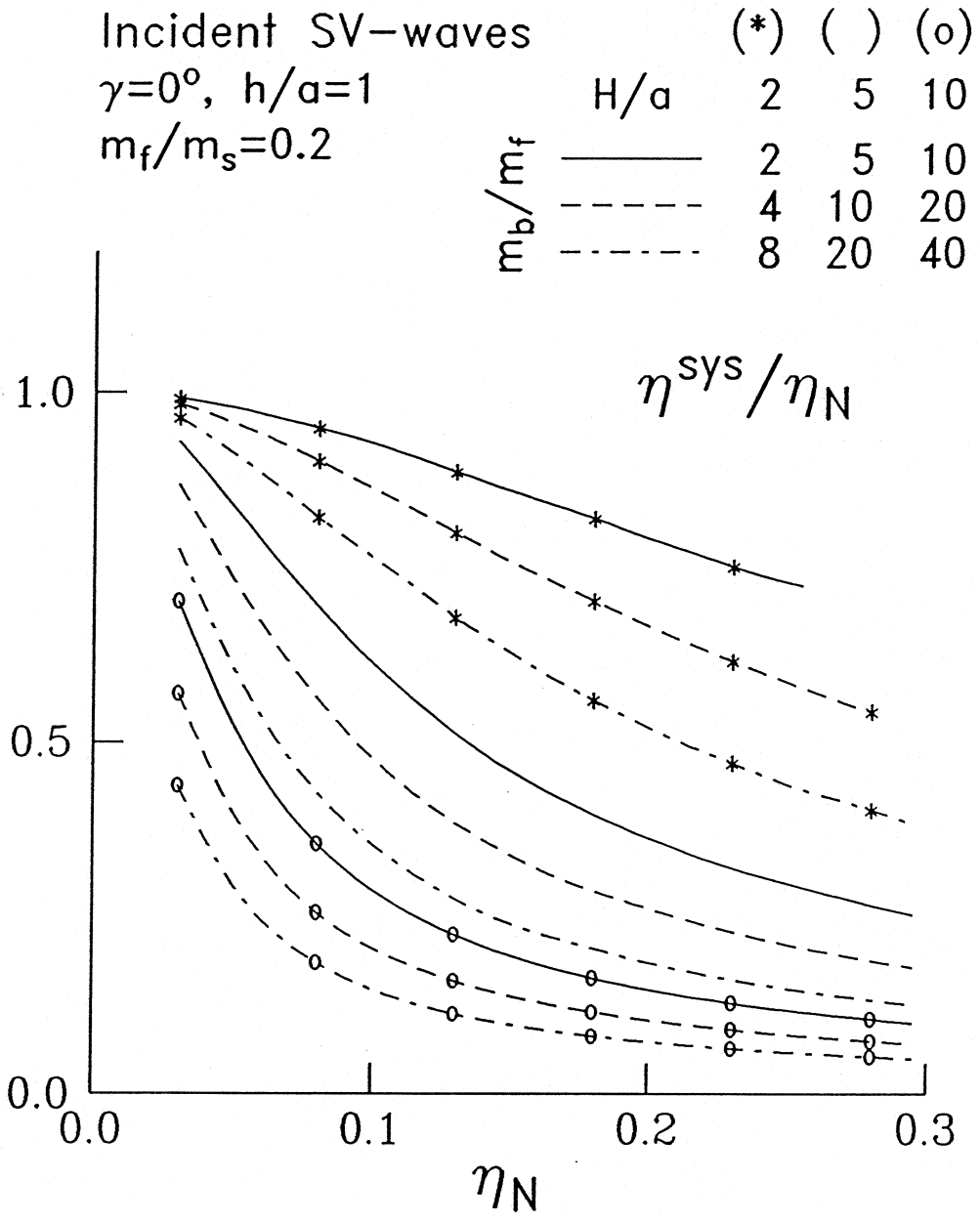

Fig. III.2.5 Reduction of the system frequency, η^{sys}/η_N for different buildings on semi-circular foundations.

of m_b/m_f cross each other, it can be concluded that it also depends on the value of the building damping whether the system will behave more like a rigid body or like a flexible structure. For $H/a = 2$ and $\eta_N = 0.05$, (Fig. III.2.2), the curves $\varsigma^{sys}(\varsigma)$ cross each other at $\varsigma \approx 0.11$, and for $H/a = 5$ and $\eta_N = 0.05$ (Fig. III.2.4) at $\varsigma \approx 0.05 - 0.06$. From this, it can be concluded that buildings with larger damping act "stirrer."

If the line $\varsigma^{sys} = \varsigma$ is drawn, it can be seen that in Fig. III.2.2 ($H/a = 2$) ς^{sys} is grater than the damping in the building. For the higher building (Fig. III.2.4), however, for sufficiently large ς the system damping ratio is lower than the damping ratio in the building.

From the curves $\varphi(\varsigma^{sys})$ in Fig. III.2.2 and III.2.4 it can be seen that for system configurations for which the structural damping affects the system response, the rocking of the base is smaller when the damping in the building is larger.

Reduction of the System Frequency, η^{sys}/η_N

The reduction of the system frequency, relative to the fixed-base frequency, is illustrated in Fig. III.2.5, where the ratio η^{sys}/η_N has been plotted versus η_N for buildings of different heights and masses ($H/a = 2$, $m_b/m_f = 2$, 4 and 8; $H/a = 5$, $m_b/m_f = 5$, 10 and 20; and ($H/a = 10$, $m_b/m_f = 10$, 20 and 40). The reduction is larger when H/a is larger and, for buildings with same height, when m_b/m_f is larger. For example, for the 10-story building ($H/a \approx 2$, and $m_b/m_f = 4$), when the shear wave velocity in the soil $\beta = 400$m/s $\eta^{sys}/\eta_N \approx 92$ %; when $\beta = 250$m/s (e.g., Los Angeles basin) $\eta^{sys}/\eta_N \approx 75$ %; and when $\beta = 50$m/s (e.g., Mexico City valley) $\eta^{sys}/\eta_N \approx 55$ %.

III.3 Effect of the Type of Incident Waves and their Incident Angle

Our results show that the frequency of the peak response η^{sys} practically does not depend on the type of incident waves and on the direction from which those waves approach the foundation, but on the material and geometric properties of the superstructure and the foundation. So does ς^{sys} if the soil is stiffer and if the system damping is small.

For incident P-waves and SV-waves with $\gamma \leq \gamma_{crit}$ (γ_{crit} is the critical angle), ς^{sys} takes on very similar values. The amplitudes of the peak response, normalized by the horizontal free-field displacement amplitude (the ratios $|u_b^{rel}|/|u^{ff}|$), are practically the same. For incident SV-waves with $\gamma > \gamma_{crit}$, the difference in ς^{sys} can be significant. The differences in the $|u_b^{rel}|/|u^{ff}|$ ratios can also be significant even for smaller η_N, as it can be seen from Fig. III.3.1 through Fig. III.3.3. For $\gamma = 45°$ $|u_b^{rel}|/|u^{ff}|$ tends to infinity for all η_N's and therefore has not been plotted. In Fig. III.3.1 through Fig. III.3.6, ς^{sys} and $|u_b^{rel}|/|u^{ff}|$ have been plotted versus η_N for buildings with $H/a = 2$, $m_b/m_f = 2$, 4 and 8, and for $\varsigma = 0.005$, 0.05 and 0.12. In the first theree of those figures the excitation is an SV-wave with incident angle $\gamma = 0°$, 20°, 30°, 45°, 60° and 85°; in the next three figures it is an incident P-wave with $\gamma = 30°$, 60° and 85°, and a vertically incident SV-wave (drawn in all

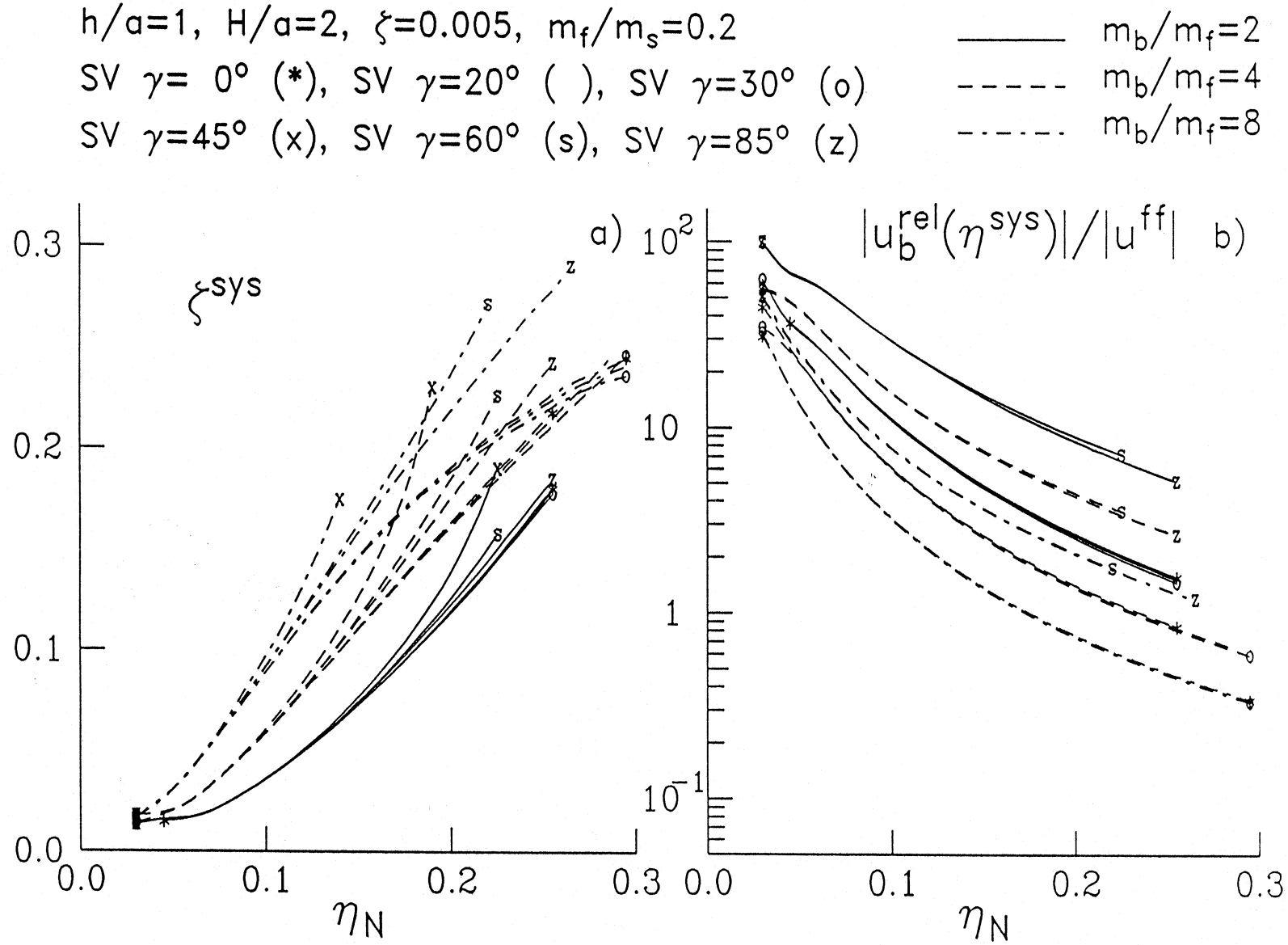

Fig. III.3.1 The system damping ζ^{sys} and the peak relative building response, $u_b^{rel}(\eta^{sys})$, normalized with the horizontal free-field surface displacement, u^{ff}, for incident plane SV-waves with incident angles $\gamma = 0°$, $20°$, $30°$, $45°$, $60°$ and $85°$ and for building damping ratio $\zeta = 0.005$.

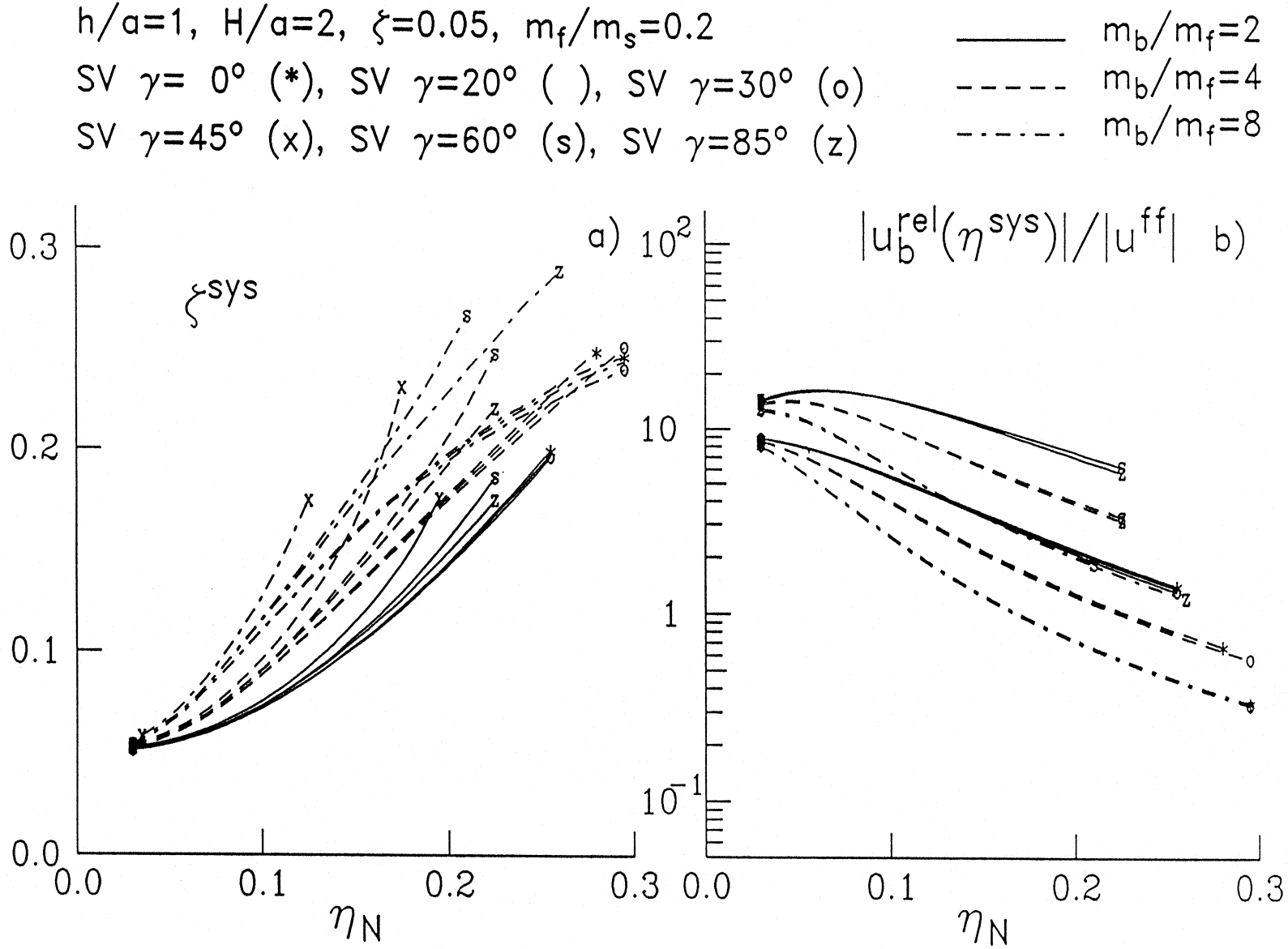

Fig. III.3.2 The system damping ζ^{sys} and the peak relative building response, $u_b^{rel}(\eta^{sys})$, normalized with the horizontal free-field surface displacement, u^{ff}, for incident plane SV-waves with incident angles $\gamma = 0°$, $20°$, $30°$, $45°$, $60°$ and $85°$ and for building damping ratio $\zeta = 0.05$.

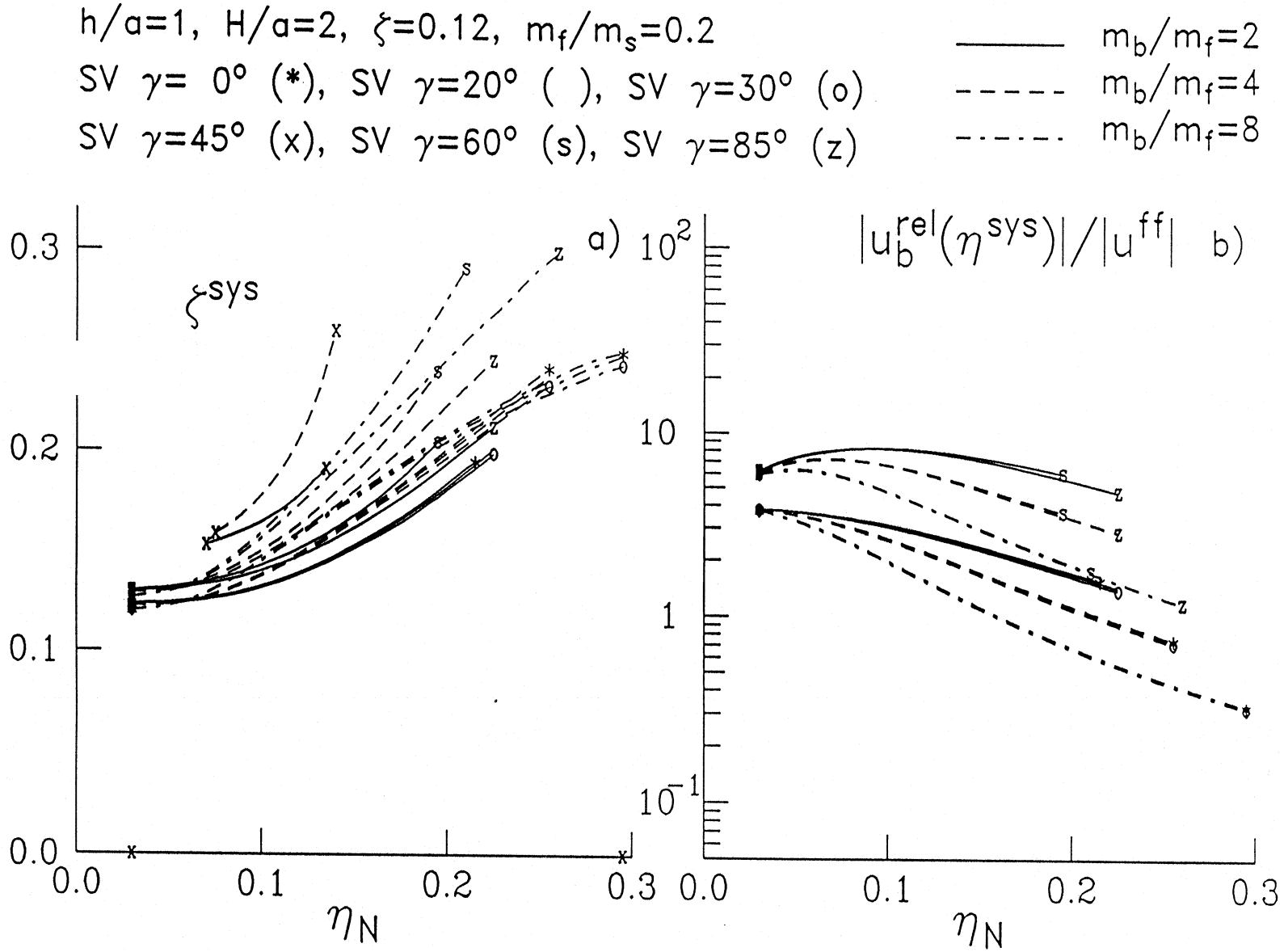

Fig. III.3.3 The system damping ς^{sys} and the peak relative building response, $u_b^{rel}(\eta^{sys})$, normalized with the horizontal free-field surface displacement, u^{ff}, for incident plane SV-waves with incident angles $\gamma = 0°$, 20°, 30°, 45°, 60° and 85° and for building damping ratio $\varsigma = 0.12$.

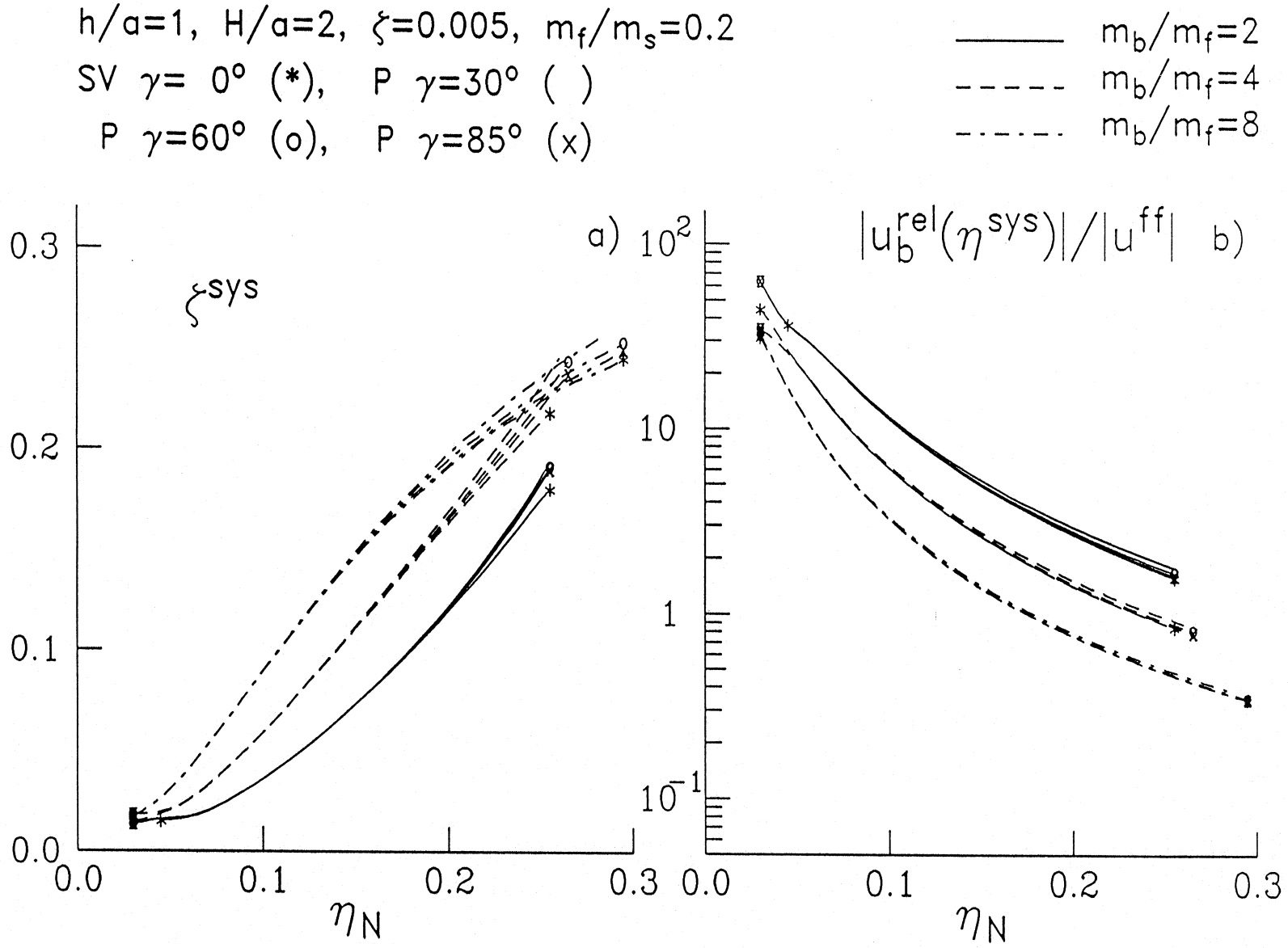

Fig. III.3.4 The system damping ς^{sys} and the peak relative building response, $u_b^{rel}(\eta^{sys})$, normalized with the horizontal free-field surface displacement, u^{ff}, for incident plane P-waves with incident angles $\gamma = 30°$, 60° and 85° and for building damping ratio $\varsigma = 0.005$.

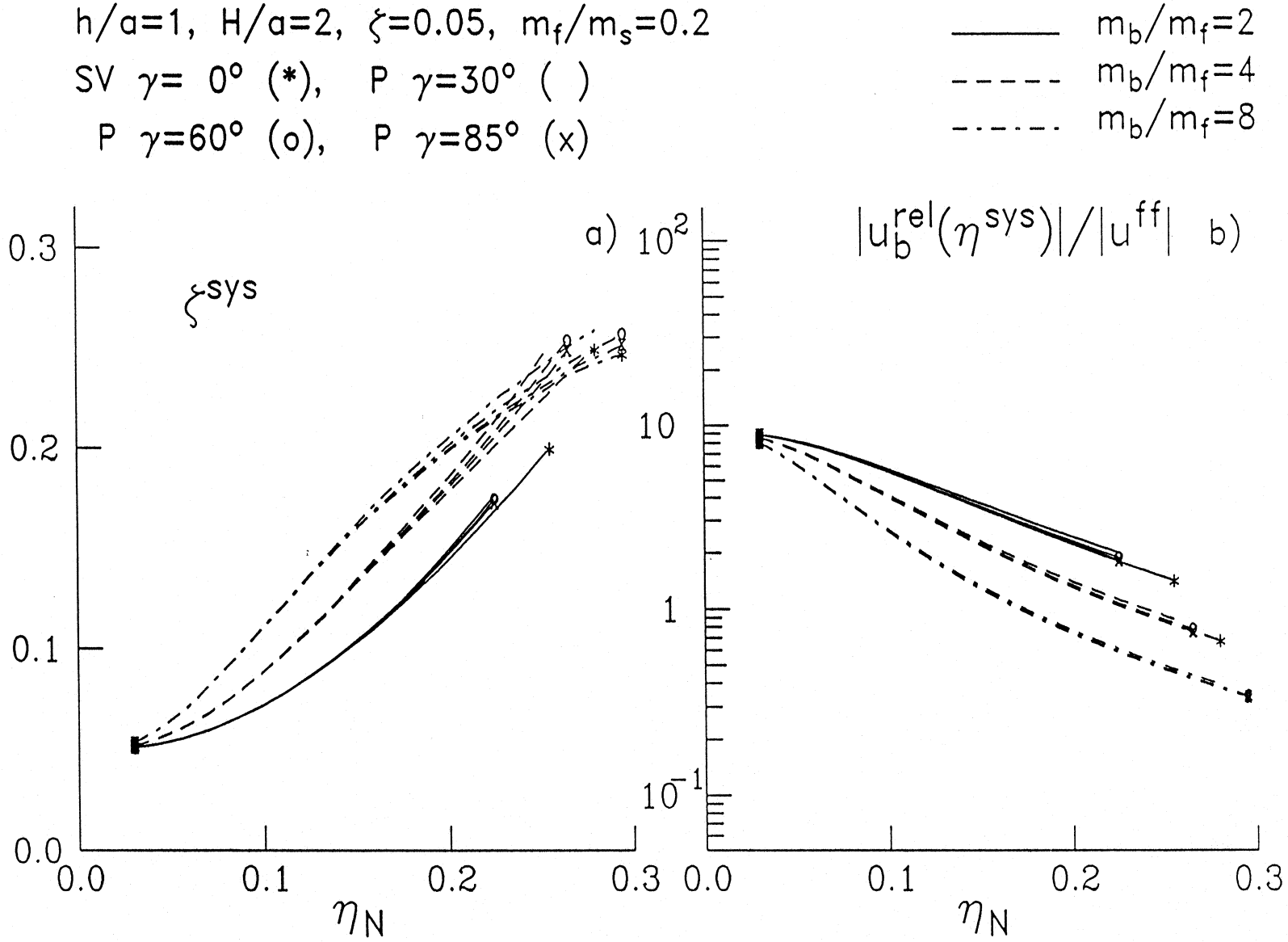

Fig. III.3.5 The system damping ς^{sys} and the peak relative building response, $u_b^{rel}(\eta^{sys})$, normalized with the horizontal free-field surface displacement, u^{ff}, for incident plane P-waves with incident angles $\gamma = 30°$, 60° and 85° and for building damping ratio $\varsigma = 0.05$.

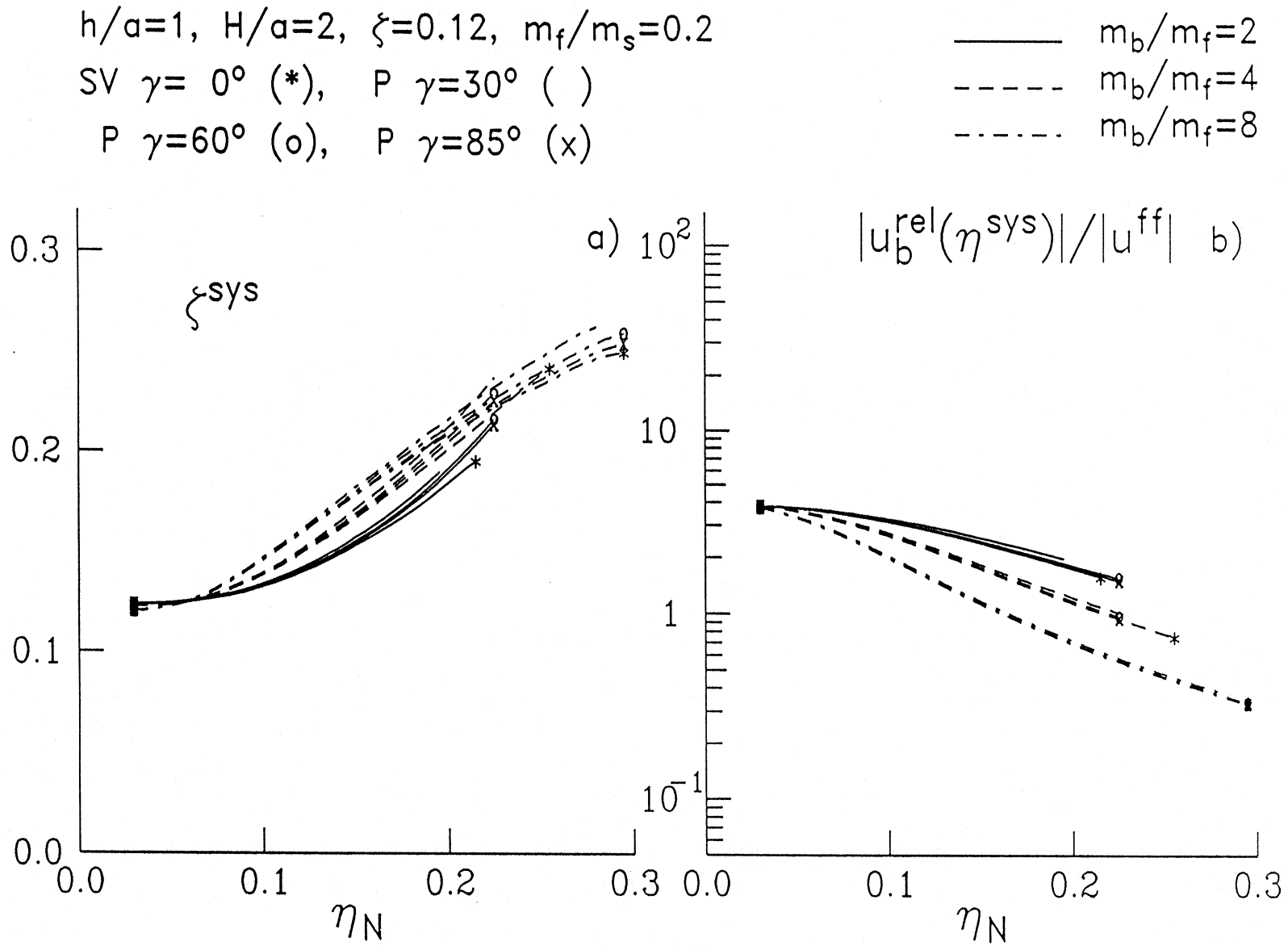

Fig. III.3.6 The system damping ς^{sys} and the peak relative building response, $u_b^{rel}(\eta^{sys})$, normalized with the horizontal free-field surface displacement, u^{ff}, for incident plane P-waves with incident angles $\gamma = 30°$, 60° and 85° and for building damping ratio $\varsigma = 0.12$.

six figures as refference). In Fig. III.3.7 and Fig. III.3.8, ς^{sys} and $|u_b^{rel}|/|u^{ff}|$ are plotted versus ς for the same buildings and excitations as in Fig. III.3.1 through Fig. III.3.3, when the stiffness of the soil is such that $\eta_N = 0.05$, and 0.2. It can be seen from these figures that the difference in ς^{sys} increases with increasing η_N (increasing flexibility of the soil) and it also increases slightly with ς. Similar behavior is observed for the higher buildings.

The reason for the dependance of ς^{sys} and $|u_b^{rel}|/|u^{ff}|$ on the type of incident waves and incident angle comes from the differences in the componenets of the the foundation input motion. The characteristics of those have been discussed in some detail in Todorovska and Trifunac (1990). What makes the case of incident SV-waves with $\gamma > \gamma_{crit}$ different from the rest of the considered excitations is the presence of considerable amount of rotation in the foundation input motion, as compared with the horizontal translation. The input base rocking represents an additional excitation to the base input translation, and it is responsible for the higher values of the ratio $|u_b^{rel}|/|u^{ff}|$. When $\gamma = 45°$ it is the only excitation, since, then, the input base translation is equal to zero. It also changes the shape of the system transfer function (e.g., causes larger relative response away from the system frequency) and, therefore, affects the system damping. It affects the phases of the base horizontal and rocking response relative to the phase of the building relative response. The base rocking is, then, a vector sum of the input rocking and the rocking due to the inertia forces of the building. From our definition of the system damping, larger ς^{sys} simply means wider peak of $|u_b^{rel}|$ and of $|\varphi|$, since η^{sys} does not depend on the type of excitation.

To illustrate the extent and the effect of this "additional" excitation, in Fig. III.3.9 the transfer function amplitude and phase of Δ, φ and u_b^{rel} have been plotted for incident SV-waves with $\gamma = 30°$ and $60°$. The model is a moderately high building ($H/a = 2$, $m_b/m_f = 4$), with low damping ($\varsigma = 0.005$) and situated on softer soil ($\eta_N = 0.2$). The system frequency is $\eta^{sys} = 0.13$. At the system frequency and for those incident angles, the amplitudes of the input base translation are $\Delta^{inp} = 2.9$ and 1.97, and of the input base rotation are $\varphi^{inp}H = 0.3$ and 1.38. The ratios $|\varphi^{inp}H|/|\Delta^{inp}| = 0.1$ and 3.9. The relative responses are $|u_b^{rel}| = 4.6$ and 2. It can be seen that the rotation amplitude $|\varphi|$ for $\gamma = 60°$ does not have a maximum at $\eta = \eta^{sys}$, but at a lower η, similar to $|\Delta|$. The shapes of the phases of Δ and φ are practically reversed for $\gamma = 30°$ and for $\gamma = 60°$. The quantity $\Delta^{inp} + \varphi^{inp}H$ would thus seem more representative for the building excitation than Δ^{inp} alone.

To illustrate how different the system response would be if the wave passage effects (kinematic interaction) are not included, in Fig. III.3.10, ς^{sys}, η^{sys}, $|u_b^{rel}(\eta^{sys})|/|u^{ff}|$ and $|\varphi(\eta^{sys})|/|u^{ff}|$ are plotted versus η_N when the foundation is driven only by a horizontal motion with amplitude $\Delta = 2$ (the solid lines). For comparison, the response to excitation by incident SV-waves with incident angles $\gamma = 0°$, $20°$, $30°$, $45°$, $60°$ and $85°$ (the dashed lines) is also shown. Different symbols are used to distinguish the lines for different incident angles. The building height is such that $H/a = 2$, the foundation is semi-circular ($h/a = 1$), the damping in the building is $\varsigma = 0.005$, and the mass ratios are $m_b/m_f = 4$ and $m_f/m_s = 0.2$. Input horizontal displacement $\Delta = 2e^{-i\omega t}$ for the foundation corresponds to excitation by vertically incident plane SV-waves of infinitely long wavelength, compared

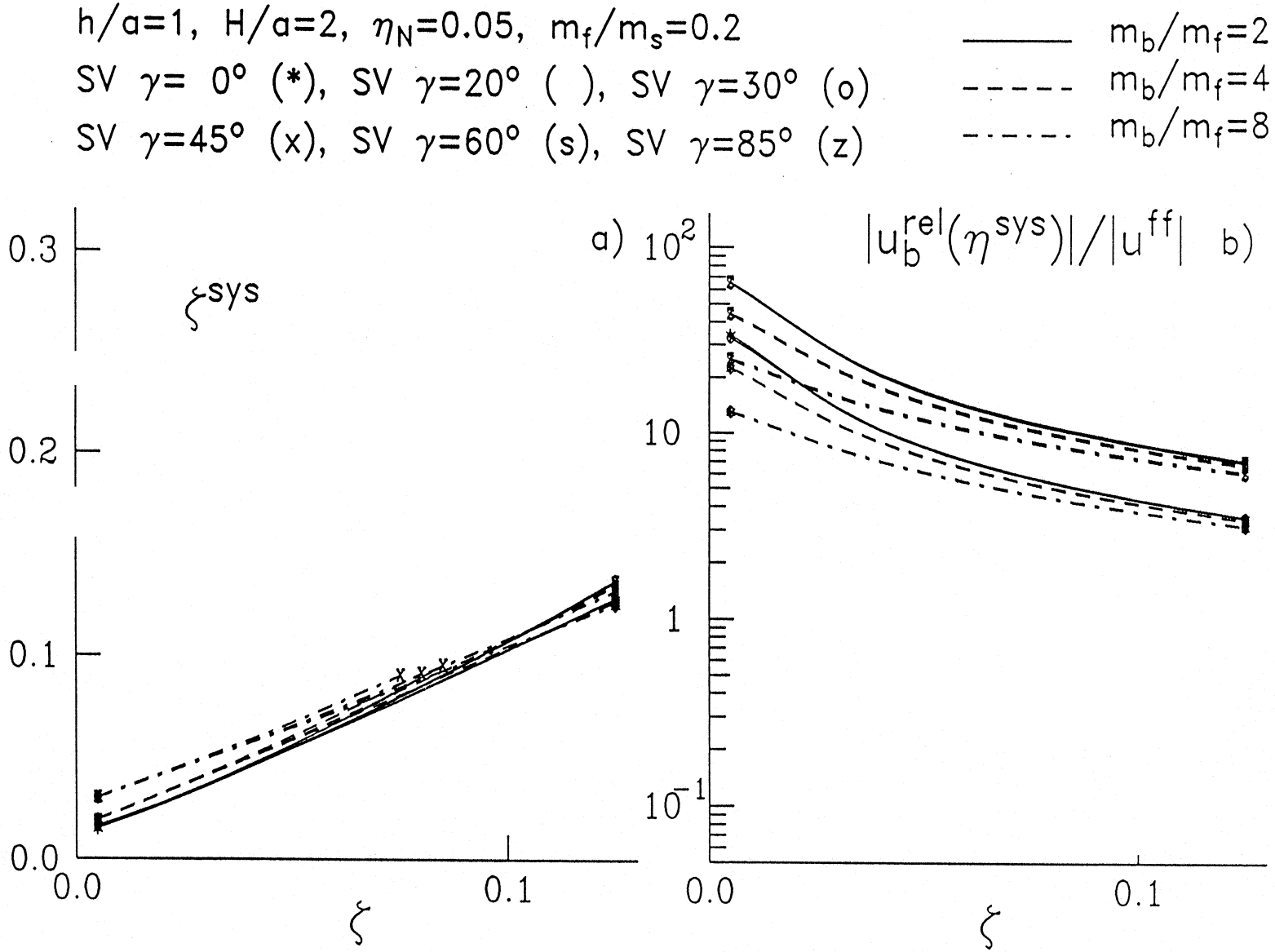

Fig. III.3.7 The system damping ζ^{sys} and the peak relative building response, $u_b^{rel}(\eta^{sys})$, normalized with the horizontal free-field surface displacement, u^{ff}, versus the damping ratio in the building, ζ, for incident plane SV-waves with incident angles $\gamma = 0°$, $20°$, $30°$, $45°$, $60°$ and $85°$ and for stiffer soil ($\eta_N = 0.05$).

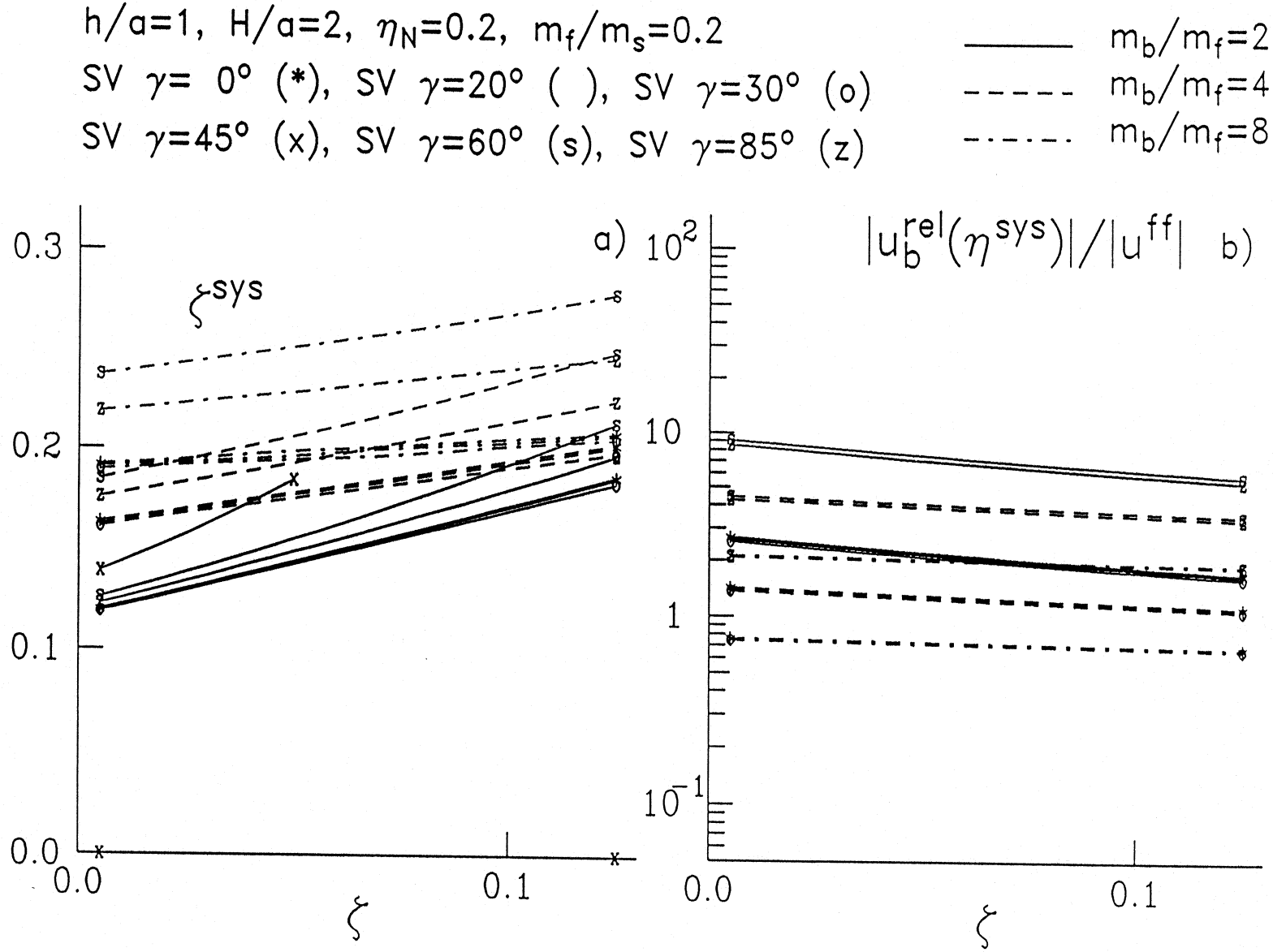

Fig. III.3.8 The system damping ς^{sys} and the peak relative building response, $u_b^{rel}(\eta^{sys})$, normalized with the horizontal free-field surface displacement, u^{ff}, versus the damping ratio in the building, ς, for incident plane SV-waves with incident angles $\gamma = 0°$, $20°$, $30°$, $45°$, $60°$ and $85°$ and for flexible soil ($\eta_N = 0.2$).

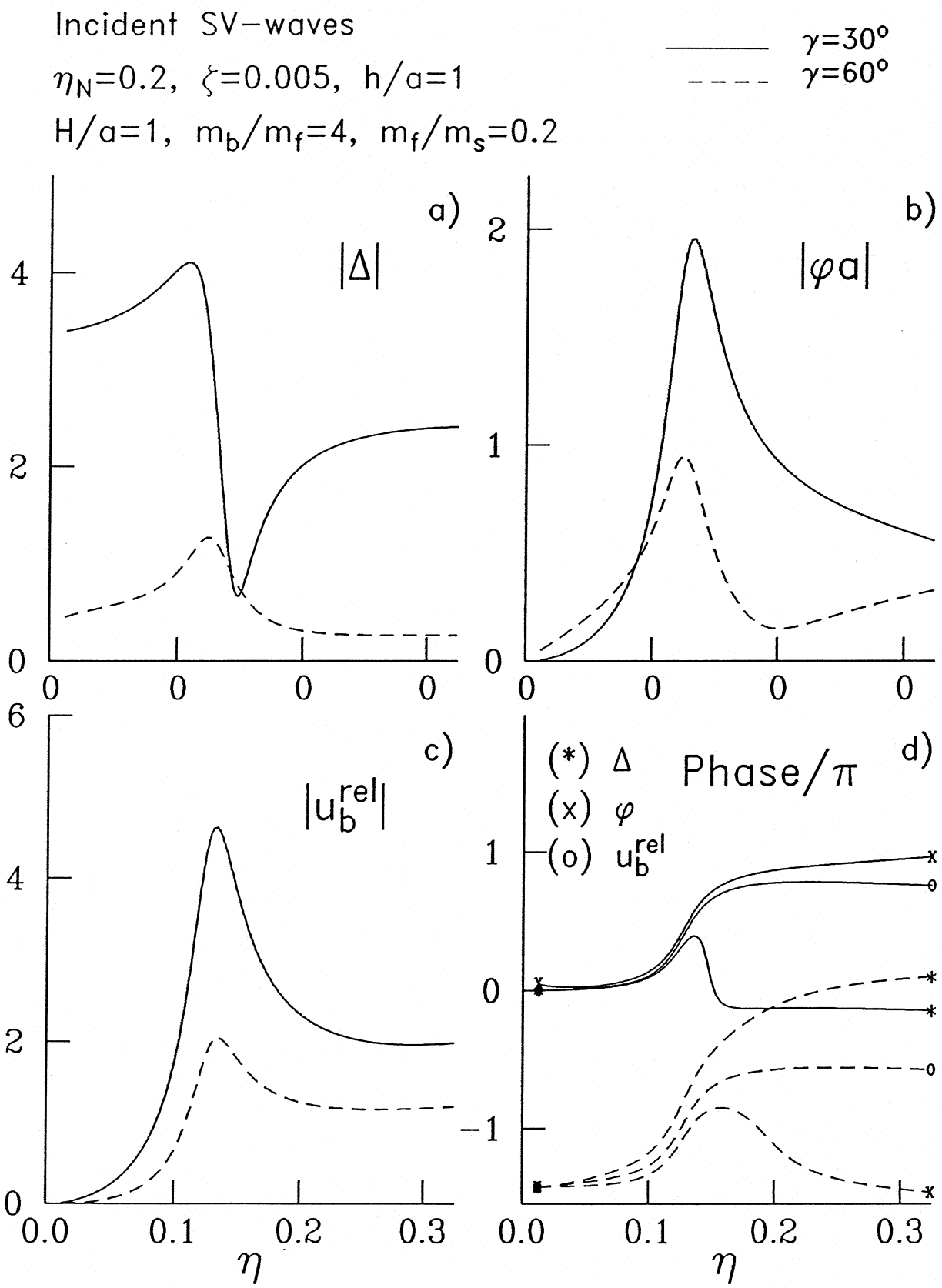

Fig. III.3.9 Transfer function amplitudes and phases of the base and of the building relative response for incident plane SV-waves with incident angles $\gamma = 30°, 60°$.

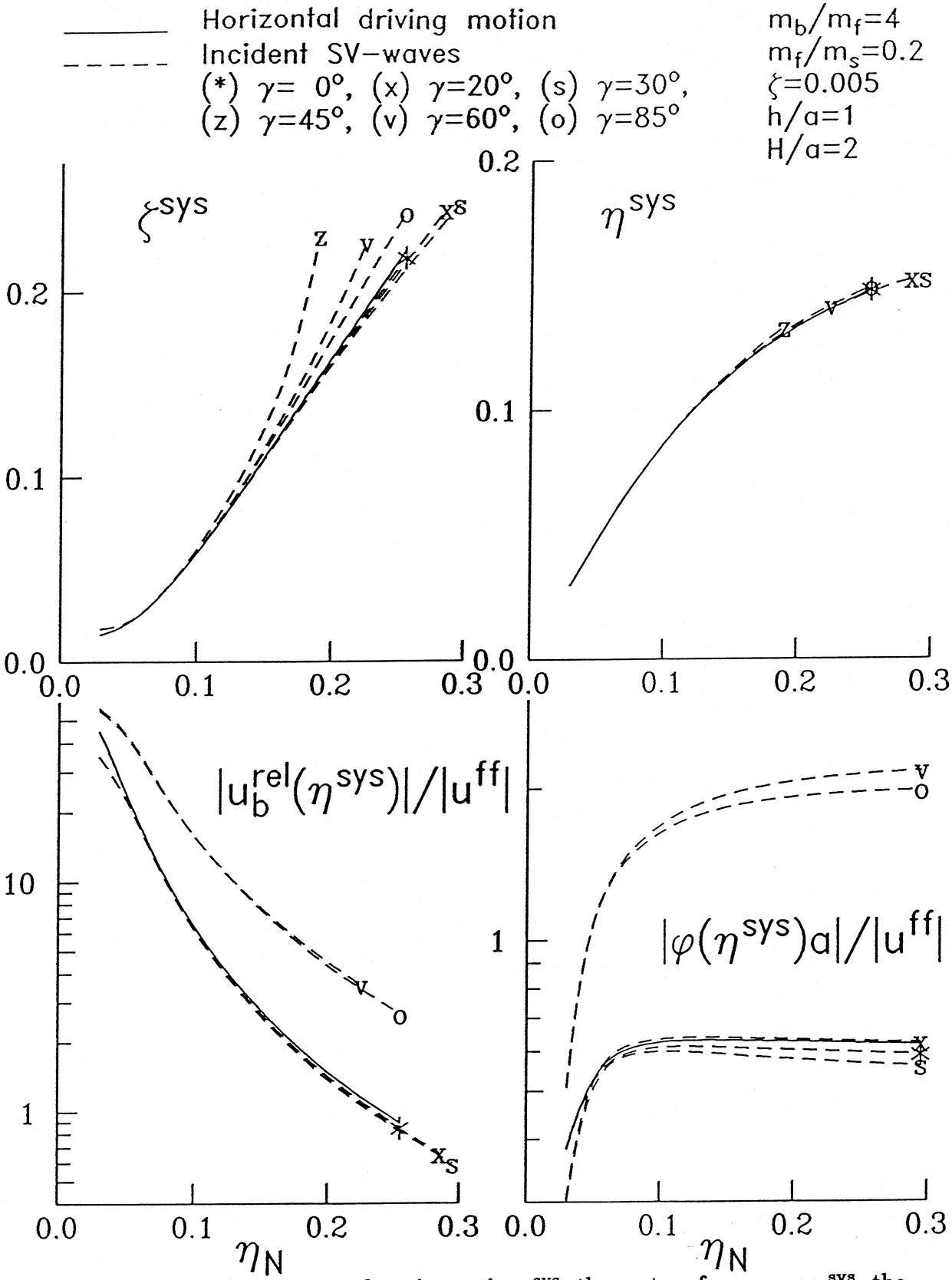

Fig. III.3.10 The system damping ratio, ζ^{sys}, the system frequency, η^{sys}, the normalized peak relative building response, $|u_b^{rel}(\eta^{sys})|/|u^{ff}|$, and the normalized peak base rocking response, $|\varphi^{rel}(\eta^{sys})a|/|u^{ff}|$, versus the relative stiffness parameter, η_N, for incident plane SV-waves (the dashed lines), and for horizontal input driving motion with constant amplitude $|u^{ff}|$ (the solid lines)

to the size of the foundation. In this approximation of the foundation input motion, the scattering of the incident waves by the foundation, and the filtering effect for shorter incident wavelengths is ignored. It can be seen from this figure that, when the wave passage effects are ignored, the system damping ratio is very close to the values for incident angles $\gamma \leq \gamma_{crit}$, but it is smaller than the values for $\gamma > \gamma_{crit}$ ($\gamma = 45°$, $60°$ and $85°$). The building relative response, normalized by the amplitude of the driving displacement, Δ, also has very similar peak amplitudes to the ones corresponding to incidence below critical angle, but significantly smaller than the peak amplitudes for incidence beyond critical angle. $|u_b^{\rm rel}(\eta^{\rm sys})|/|u^{ff}|$ and $|\varphi(\eta^{\rm sys})|/|u^{ff}|$ are not plotted for $\gamma = 45°$, because for this incident angle $|u^{ff}| = 0$. The peak rocking response, normalized by $|u^{ff}|$, also has similar amplitudes to the case for incidence below critical angle, but noticeably smaller amplitudes than for incidence beyond critical angle. This means that, for incident angles below critical angle, most of the base rotation comes from the inertia forces of the building. It can be concluded that, if the wave passage effects are excluded from the analyses, by assuming simplified excitation, the system damping ratio, and the amplitudes of the system response, may be underestimated. These effects appear to be caused by the inhomogeneous part of the free-field motion, for incident angles grater than the critical angle. For incident plane P-waves, the same conclusions hold as for incident plane SV-waves below critical angle.

III.4 Effects of the Depth of the Embedment

To illustrate the effects of the depth of the embedment, the results are presented in the following form. The system damping, $\varsigma^{\rm sys}$, the system frequency, $\eta^{\rm sys}$, normalized by the fixed-base frequency η_N, the peak amplitude of the building relative response, $|u_b^{\rm rel}(\eta^{\rm sys})|$, and the peak amplitude of the base rocking response, $|\varphi(\eta^{\rm sys})|$, are plotted versus h/a, or versus η_N. The translation of the foundation is not shown and discussed. The ratio $\eta^{\rm sys}/\eta_N$ is an indicator of the reduction of the system frequency as a result of the flexibility of the soil.

In Fig. III.4.1 and Fig. III.4.2, $\varsigma^{\rm sys}$, $\eta^{\rm sys}/\eta_N$, $|u_b^{\rm rel}(\eta^{\rm sys})|$ and $|\varphi(\eta^{\rm sys})a|$ have been plotted versus h/a ($0.5 \leq h/a \leq 1$), for a building with height $H/a = 2$, and excited by a vertically incident plane SV-wave. (γ appearing in these figures is the incident angle, measured from the normal to the half-space surface to the direction of wave propagation). The curves without symbols are for $\eta_N = 0.1$, and with the symbols, for $\eta_N = 0.06$. The foundation is taken to be massless, in order to eliminate the effects of the change of its mass as the shape of the foundation changes. The solid line and the different segmented lines correspond to three values of the building mass, which is expressed in terms of $m_{s,1}$, the mass replaced by a semi-circular foundation of width $2a$. The ratio $m_b/m_{s,1}$ =0.4, 0.8 and 1.6; the value $m_b/m_{s,1}$ =0.8 corresponds to the typical value of ρ_b/ρ_s. The models in these two figures differ only in the value of the damping in the building; in Fig. III.4.1, $\varsigma = 0.005$, and, in Fig. III.4.2, $\varsigma = 0.05$. It can be seen from the results in these figures that, as the depth of the foundation decreases, the reduction of the system frequency, relative to the fixed-base frequency, increases, meaning that deeper foundations act "stiffer." The relative response is larger when the foundation is deeper; it is larger when the damping in the building is smaller (Fig. III.4.1). The system damping ratio, in both figures, is larger

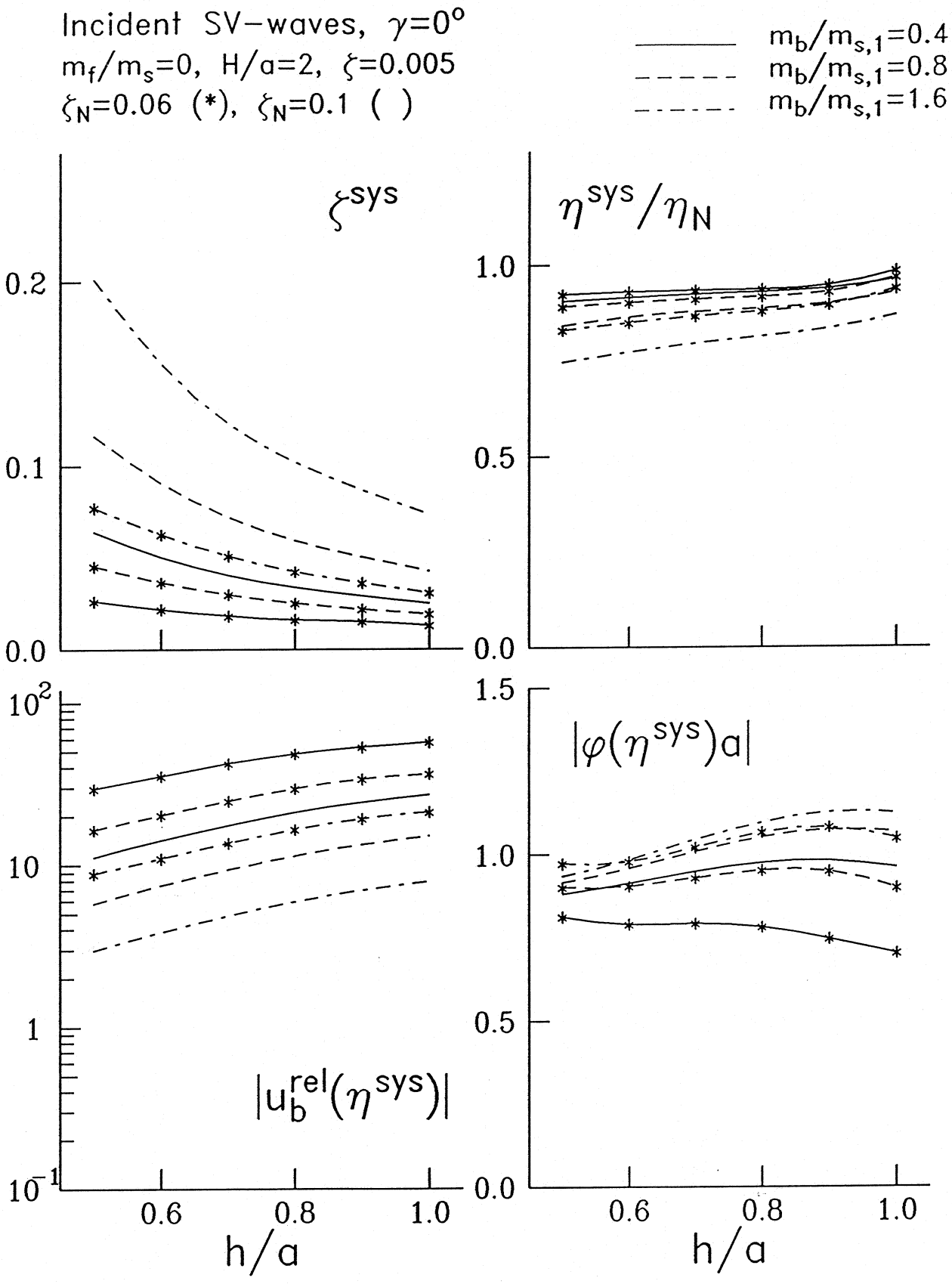

Fig. III.4.1 Dependance of the system parameters and the system response on the depth of the embedment for $\zeta = 0.005$, $\eta_N = 0.06$ and 0.1 and when the foundation is massless.

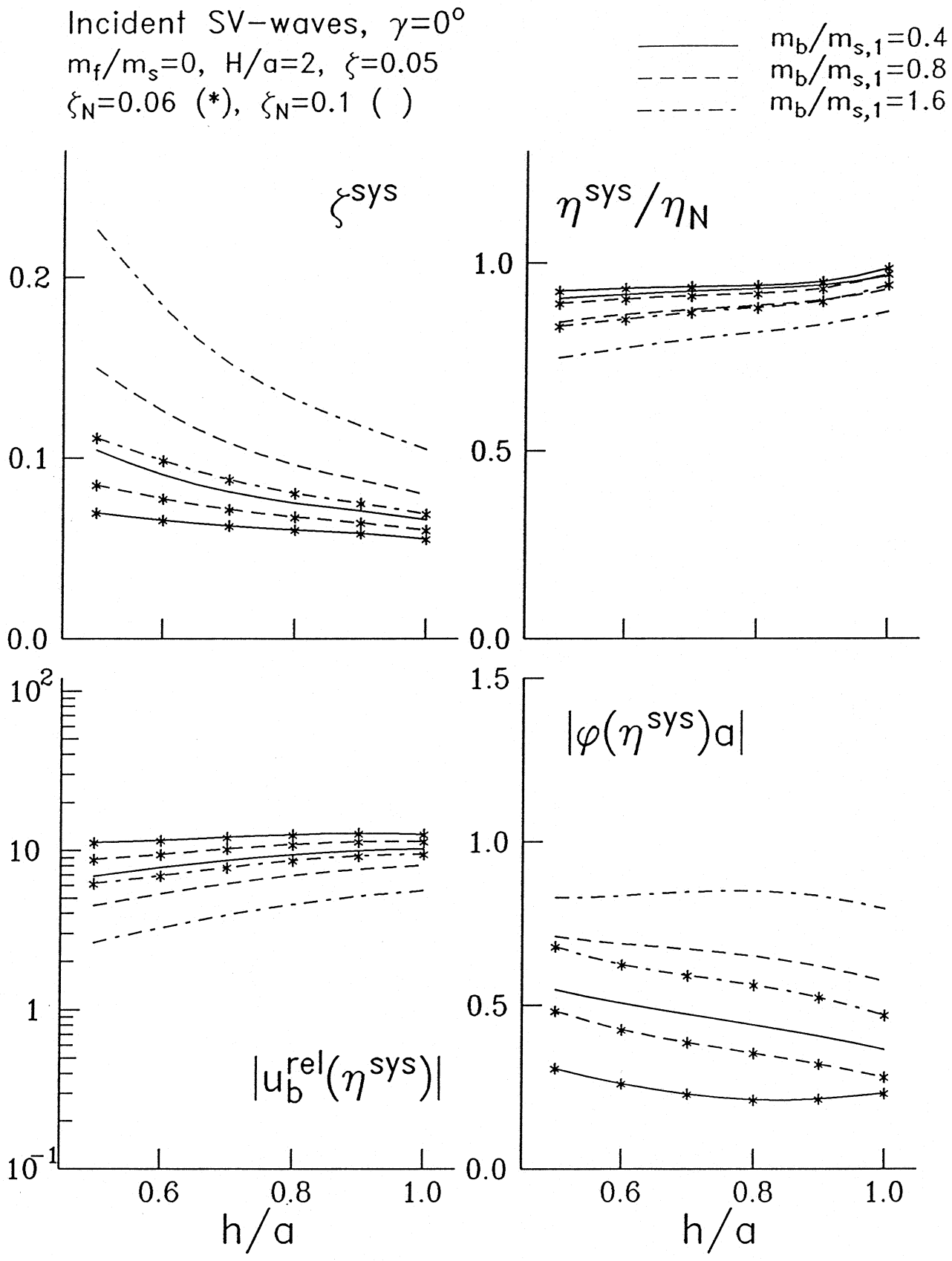

Fig. III.4.2 Dependance of the system parameters and the system response on the depth of the embedment for $\zeta = 0.05$, $\eta_N = 0.06$ and 0.1 and when the foundation is massless.

when the foundation is deeper, when the building is heavier, and when the damping in the building is larger. In Fig. III.4.1, the amplitude of the base rocking, in most of the cases, is larger when the foundation is deeper; it is smaller only for the lightest building and on stiffer soil. In Fig. III.4.2, the base rocking is smaller for deeper foundations.

In Fig. III.4.3 and Fig. III.4.4, ς^{sys}, η^{sys}, $|u_b^{rel}(\eta^{sys})|$ and $|\varphi(\eta^{sys})a|$ are plotted versus the relative stiffness parameter η_N, for a building with $H/a = 2$. The curves marked with different symbols correspond to foundations with different depth ("*" correspond to $h/a = 1$, and "o" to $h/a = 0.5$). The density of both foundations is same ($m_f/m_s = 0.2$). The deeper foundation is heavier by a factor of approximately 2, because its cross-sectional area is approximately twice as large as the cross-sectional area of the foundation with the smaller depth. The different types of lines correspond to different values of m_b/m_f. The lines of same type correspond to approximately same value of the building mass. $m_b/m_f = 2$, 4 and 8 for the deeper foundation, and $m_b/m_f = 4$, 8 and 16 for the shallow foundation. (the ratio m_b/m_f differs for the two foundations, because of the difference in their mass). The values $m_b/m_f = 4$ when $h/a = 1$, and $m_b/m_f = 8$ when $h/a = 0.5$, correspond to the "typical" value of the ratio ρ_b/ρ_s. The models in these two figures differ only by the value of the building damping; in Fig. III.4.3, $\varsigma = 0.005$, and, in Fig. III.4.4, $\varsigma = 0.05$. In Fig. III.4.5 and Fig. III.4.6, the same quantities are shown as in Fig. III.4.3 and Fig. III.4.4, but for higher buildings ($H/a = 5$). In these figures, $m_b/m_f = 5$, 10 and 20 when $h/a = 1$, and $m_b/m_f = 10$, 20 and 40 when $h/a = 0.5$. The foundation mass is as in Fig. III.4.3 and Fig. III.4.4. In Fig. III.4.5, $\varsigma = 0.005$, and, in Fig. III.4.6, $\varsigma = 0.05$. It can be seen from these figures that for stiffer soil (lower η_N), the system damping ratio, the system frequency and the relative building response do not depend much on the depth of the embedment and on the building mass. As $\eta_N \to 0$, $\varsigma^{sys} \to \varsigma$, $\eta^{sys} \to \eta_N$, and the relative response goes to the fixed-base response. As the soil becomes softer (η_N increases), both for $h/a = 1$ and for $h/a = 0.5$, the system frequency decreases, the relative response decreases, and the system damping ratio increases. For the lower and lighter buildings (Fig. III.4.3 and Fig. III.4.4), the base rocking increases as the soil becomes more flexible, approaching the asymptotic value for a rigid building. For the higher and heavier building (Fig. III.4.5 and Fig. III.4.6), the rocking amplitudes approach the asymptotic value for a rigid building in some cases from above and in some cases from below, depending on the maximum amplitude they have reached for smaller values of η_N. For a given value of η_N, the system frequency is smaller when the embedment depth is smaller, as it is the case in Fig. III.4.1 and Fig. III.4.2. The peak relative response is smaller when the embedment depth is smaller in all the four figures. In all the four figures, and in all except one case, the system damping ratio ς^{sys} is larger when the embedment depth is smaller. Also, with the same exception, when the soil is stiffer, the base rocking is smaller for buildings on deeper foundations, and when the soil is softer, it is larger for buildings on deeper foundations. The exception case is the heaviest building in Fig. III.4.5 and Fig. III.4.6, ($H/a = 5$, and $m_b/m_f = 20$ and 40 for $h/a = 1$ and 0.5 respectively).

The building mass also affects the system response. The results in this report show that, for given η_N, the system frequency is lower and the relative response is also lower, when the building mass is larger. (From Eq. (III.2), it follows that, for a given value

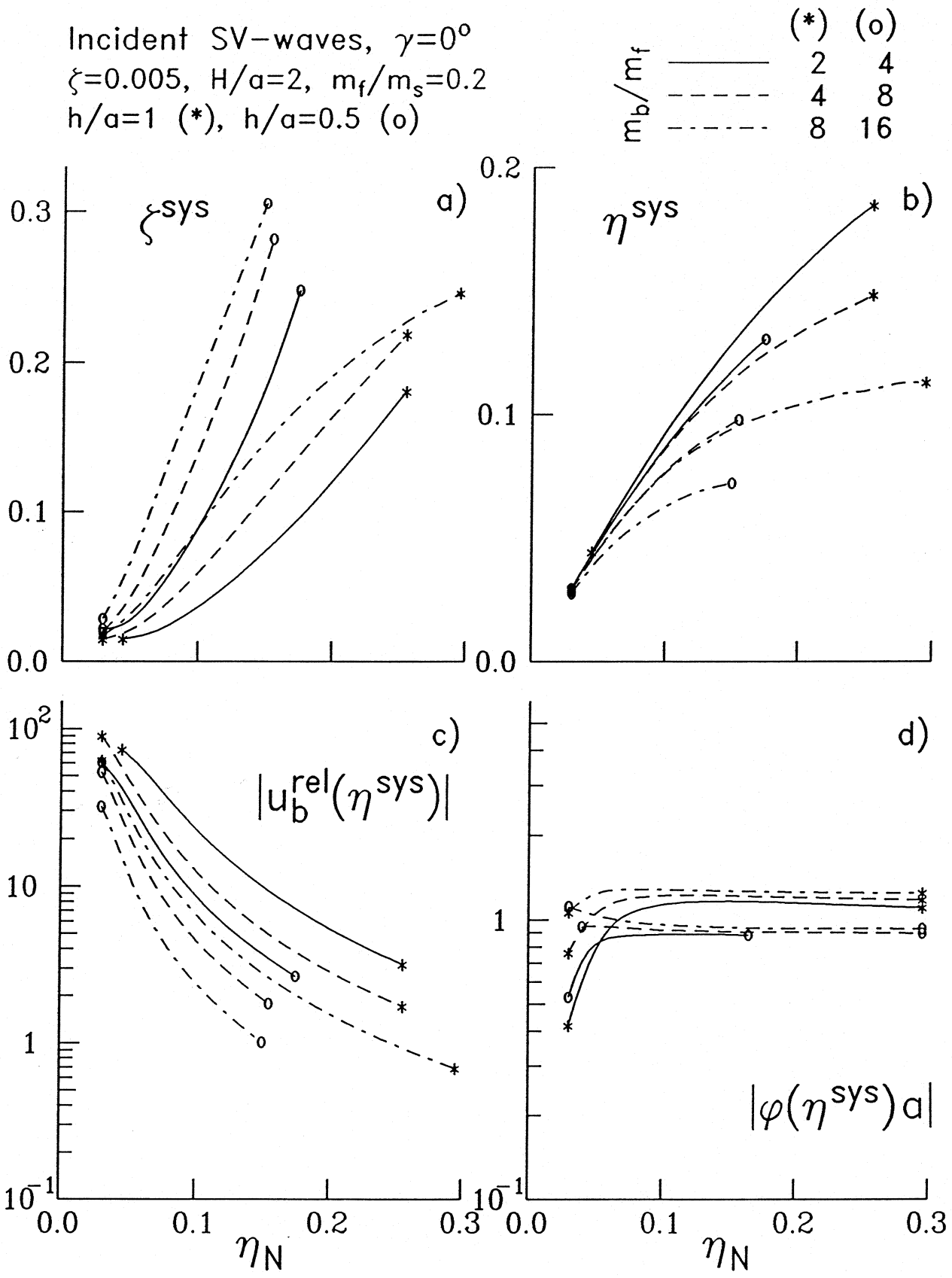

Fig. III.4.3 The system parameters and the system response versus η_N for medium high buildings ($H/a = 2$) with damping ratio $\zeta = 0.005$, on semi-circular and on shallow foundations ($h/a = 1$ and 0.5).

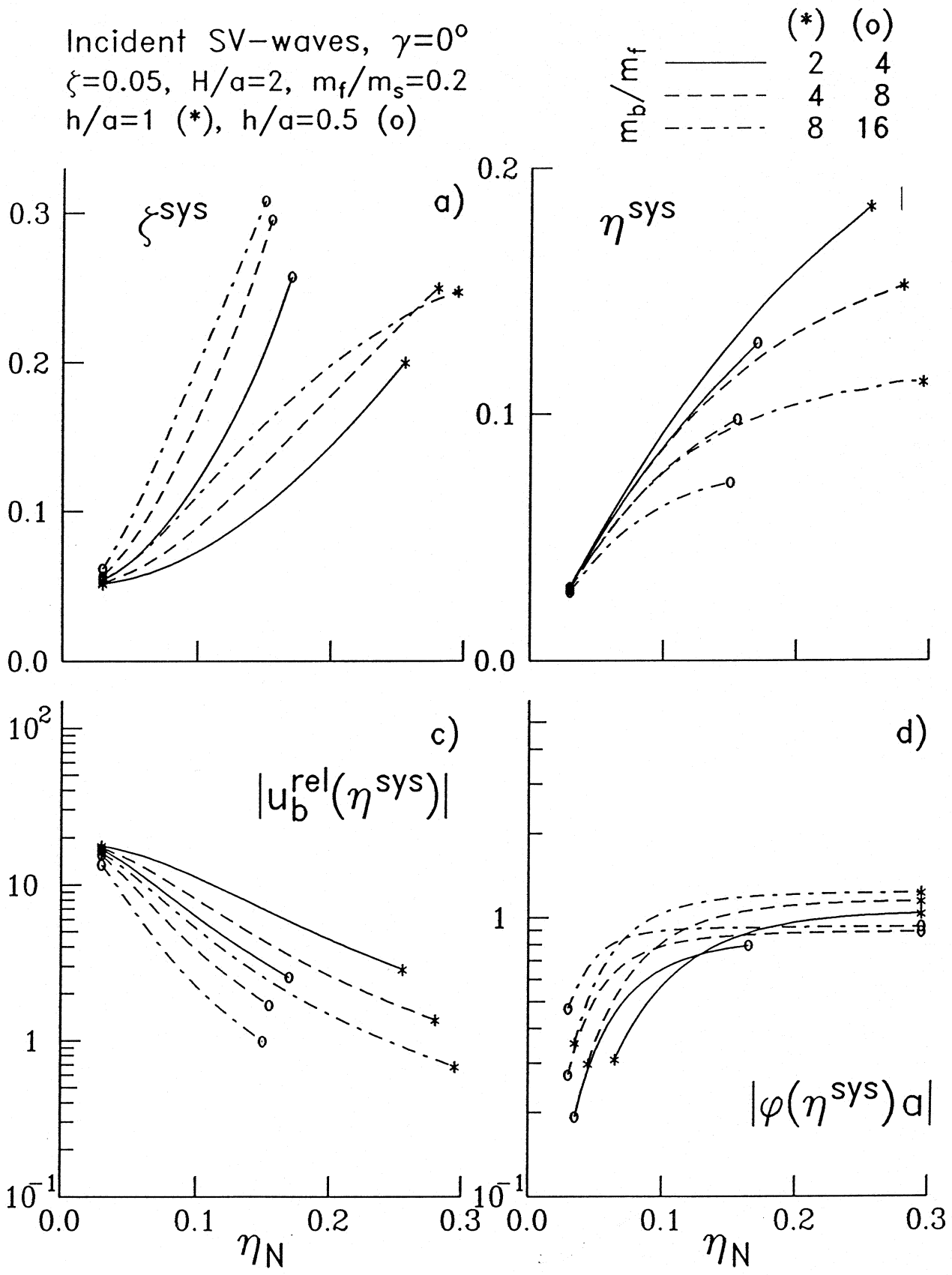

Fig. III.4.4 The system parameters and the system response versus η_N for medium high buildings ($H/a = 2$) with damping ratio $\zeta = 0.05$, on semi-circular and on shallow foundations ($h/a = 1$ and 0.5).

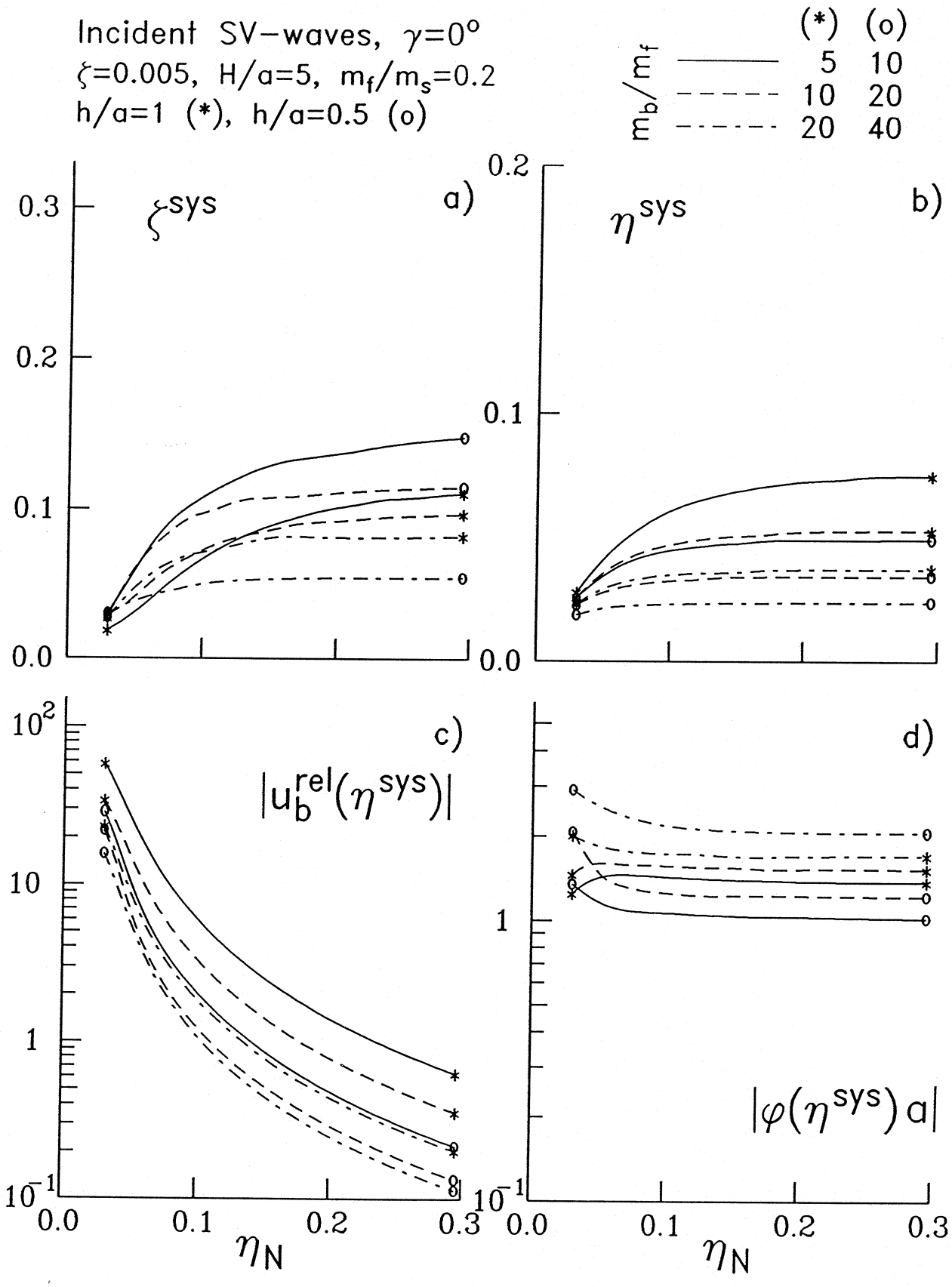

Fig. III.4.5 The system parameters and the system response versus η_N for higher buildings ($H/a = 5$) with damping ratio $\zeta = 0.005$, on semi-circular and on shallow foundations ($h/a = 1$ and 0.5).

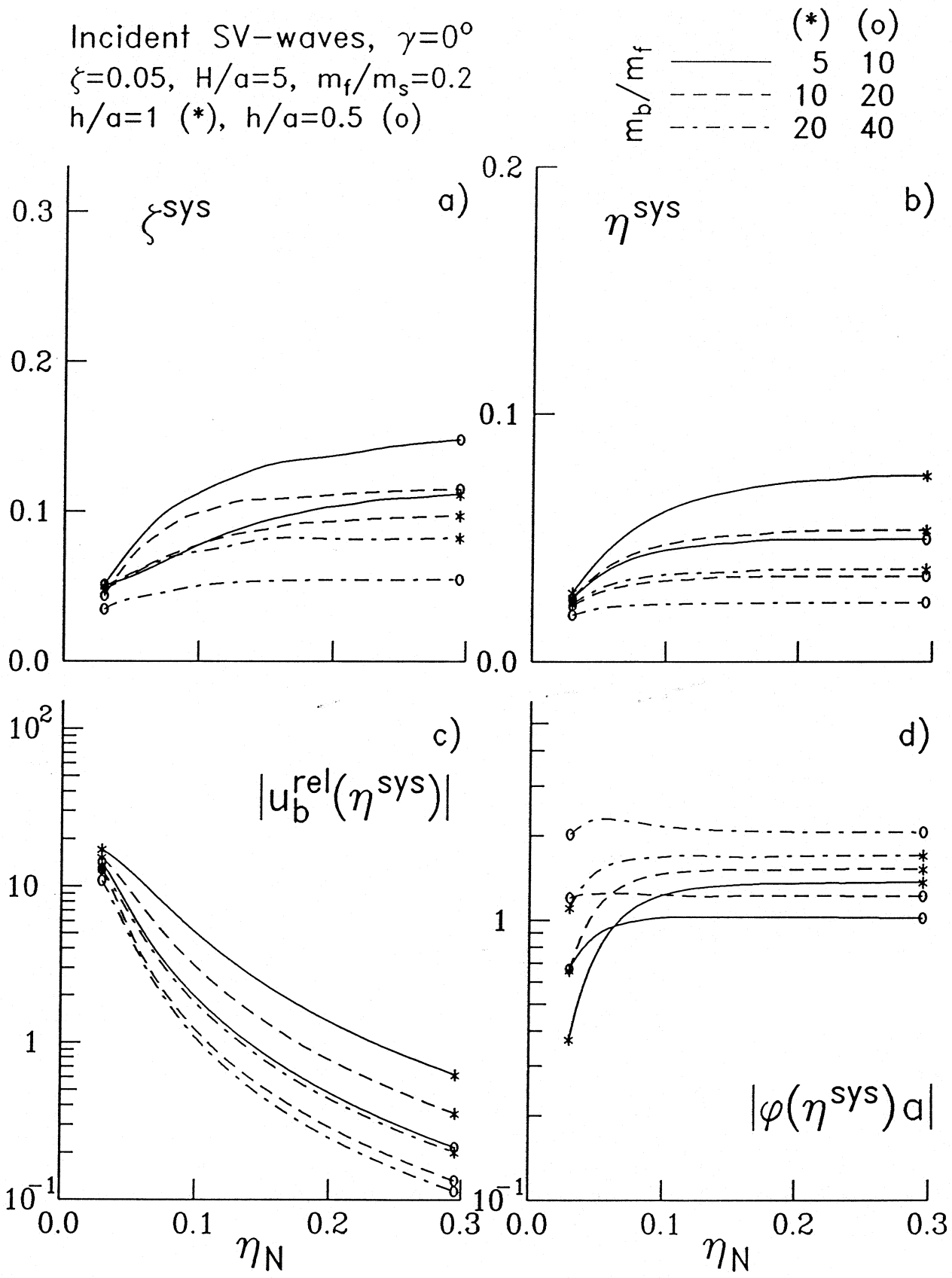

Fig. III.4.6 The system parameters and the system response versus η_N for higher buildings ($H/a = 5$) with damping ratio $\zeta = 0.05$, on semi-circular and on shallow foundations ($h/a = 1$ and 0.5).

of η_N, larger value of m_b/m_s implies larger value of the static stiffness ratio $\frac{K_b}{\mu a}$). The system damping ratio (measured using Eq. (III.1)), however, may be smaller or larger depending on the "apparent" stiffness of the soil. Two regimes of the system behavior can be distinguished, depending on the apparent stiffness of the soil. In Regime I, the soil is stiffer and the building natural frequency and damping influence more significantly the system response. In Regime II, the soil is so flexible that the system behaves almost like a rigid body embedded in the elastic half-space. From the results in Fig. III.4.3 through Fig. III.4.6, it can be seen that, for given value of η_N, if the system response is governed by Regime I, the system damping is larger when the building mass is larger, while, if it is governed by Regime II, it is smaller when the building mass is larger. The value of η_N at which the transition between the two regimes occurs is smaller when the building is higher and heavier, and when the damping in the building is larger. This value also depends on the shape of the foundation, which affects its stiffness. From Fig. III.4.5 and Fig. III.4.6, it can be seen that, the curves for different values of the building mass intersect each other at smaller value of η_N when the foundation depth is smaller. This means that buildings on shallow foundations enter Regime II at lower values of η_N than buildings on deeper foundations.

The real parts of the entries of the foundation impedance matrix are commonly called foundation stiffness coefficients, while the imaginary parts, normalized by the dimensionless frequency $a_0 = \pi\eta = \frac{\omega_N a}{\beta}$, are referred to as radiation damping coefficients. For the circular foundations used in this report (2D), both the stiffness coefficients and the radiation damping coefficients are smaller when the embedment depth is smaller. However, the oscillator relative response and the system damping ratio depend not only on the radiation damping coefficients but also on the relative stiffness of the soil. For example, when there is no material damping in the soil, the relative response is smaller, and the system damping ratio is larger (Bielak, 1975), when η_N is larger. The foundation shape also affects the apparent stiffness of the soil. Deeper foundations act "stiffer" and this may explain why the relative response in Fig. III.4.1 through Fig. III.4.6 is larger for buildings on deeper foundations, in spite of the fact that the radiation damping coefficients are larger for deeper foundations.

The system damping ratio depends (1) on the radiation damping coefficients, which control the width of the peak in the transfer-function, and (2) on the overall stiffness of the foundation, which controls the frequency of the peak. (From Eq. (13) it can be seen that of two peaks with same width, the one at lower frequency will have larger damping ratio.) These two factors compete in their influence on the system damping ratio. The system frequency is lower when the foundation depth is smaller, but on the other hand, the radiation damping coefficients are then smaller. In the 2D model analyzed in this report, as can be concluded from the presented results, except for very heavy and tall buildings, the first factor prevails, and the system damping ratio is larger when the foundation depth is smaller.

Larger reduction of the building relative response (because of smaller soil stiffness) is usually associated with larger rocking of the base. This is the case for lower η_N. Then, the

base rocking is larger when the building foundation has smaller depth, as it can be seen from Fig. III.4.3 through Fig. III.4.6. However, for larger η_N, the base rocking is smaller for a foundation with smaller depth. This may be because the foundation driving forces may be smaller when the foundation depth is smaller. The explanation is the following. The peak of the transfer-function in all the presented results is in the interval $\eta \in (0, 0.2)$. Values of η in this interval correspond to long incident waves, compared with the size of the foundation, for which the stresses in the soil do not vary much along the contact surface with the foundation. The foundation driving forces are integrals of the stresses along the contact surface, and, for long incident waves, they may be larger for deeper foundations for which the contact area with the soil is larger.

III.5 Analytical Expressions for the System Frequency and the System Damping Developed by other Authors

As mentioned in the introduction, previous works on damping during soil-structure interaction usually do not include the kinematic interaction, but some do include the material damping in the soil. Functional relationships between the system parameters were developed by Bielak (1971, 1976) and in Luco (1980). Our empirically determined curves for the system damping as a function of the relative stiffness parameter η_N for the building with $H/a = 2$ are very similar to the curves obtained by their analytical expressions. In terms of our dimensionless parameters, their equations for the system frequency and for the system damping are the following

$$\frac{1}{(\eta^{\text{sys}})^2} = \frac{1}{\eta_N^2} + \frac{1}{\eta_R^2} + \frac{1}{\eta_H^2}, \qquad (III.3)$$

where η_R and η_H are the rocking and the horizontal frequencies, in terms of the dimensionless frequency η, and

$$\varsigma^{\text{sys}}(\eta^{\text{sys}}) = \left(\frac{\eta^{\text{sys}}}{\eta_N}\right)^3 \varsigma + \left[1 - \left(\frac{\eta^{\text{sys}}}{\eta_N}\right)^2\right] \varsigma_s + \left(\frac{\eta^{\text{sys}}}{\eta_H}\right)^3 \varsigma_H + \left(\frac{\eta^{\text{sys}}}{\eta_R}\right)^3 \varsigma_R \qquad (III.4)$$

where ς_s, ς_H and ς_R are the material soil, the horizontal and the rocking damping ratios. From Eq. (III.3) it follows that as the soil flexibility increases, i.e. as $\eta_N \to \infty$, $\eta^{\text{sys}} \to \eta^{\text{rig}}$ which satisfies

$$\frac{1}{\eta^{\text{rig}^2}} = \frac{1}{\eta_R^2} + \frac{1}{\eta_H^2} \qquad (III.5)$$

As the soil becomes very stiff (i.e. as $\eta_N \to 0$), $\eta^{\text{sys}} \to \eta_N$. The participation factors for the different damping ratios in the equation for ς^{sys} depend on how close η^{sys} is to η_N or to η^{rig}. The contribution of ς is the largest when the soil is very stiff, and it decreases as the soil becomes more flexible. The opposite holds for the participation factors of ς_s, ς_H and ς_R.

III.6 Comparison with Results of 3D Models

Most similar 3D model to the 2D model analyzed in this report is a SDOF oscillator with rocking and torsional springs and dampers, supported by a hemispherical rigid foundation embedded into a homogeneous half-space (Lee, 1979) (both models are analytical, for oval foundation shape, and include the wave passage effects). Excited by in-plane excitation, this 3D model will respond with motion with the same degrees-of-freedom as the 2D model in this report.

Other similar model, analyzed by Bielak (1975), is a SDOF structure on a rectangular prismatic foundation embedded into an elastic layer over a half-space and excited by horizontal motion at the base with constant amplitude. This model overestimates the horizontal translation, but neglects the rotation of the foundation input motion. The coupling terms in the foundation impedance matrix, between the horizontal and the rocking motion are neglected, and the soil stiffness and the radiation damping are modeled by two pairs of a spring and a dashpot - one pair for the horizontal motion and the other pair for the rocking motion. This model does include the damping in the soil. To input horizontal motion of the base, this model will also respond with motion in the $x-z$ plane, as the 2D model in this report.

The three models agree in that the system frequency is reduced more for larger values of η_N, and for higher buildings. The results for the 2D model in this report agree with the results for the semi-spherical foundation (Lee, 1979) in that, for given values of η_N and H/a, larger building mass causes larger reduction of the system frequency and of the relative response. This is also in agreement with the results for 2D building models on circular 2D foundations excited by plane SH waves (Trifunac and Wong, 1974; Trifunac, 1972), but is in contradiction with the results in Bielak (1975), for the prismatic foundations embedded in soil with hysteretic damping.

Comparison of the system damping ratios in 2D and 3D for embedded foundations of different depth is possible only between the 2D model in this report and the model in Bielak (1975). The results of both models agree in that, for deeper foundations, the stiffness and radiation damping coefficients are larger, and that the reduction of the system frequency is larger when the embedment depth is smaller. However, there is a disagreement in the results for the system damping ratio and the overall damping effect of the interaction. For the 2D model, the relative response is reduced more when the foundation depth is smaller, and the system damping ratio, except for the very heavy building in Fig. III.4.5 and Fig. III.4.6, is larger when the depth of the foundation is smaller. For the 3D model (Bielak, 1975), it has been concluded that the system damping ratio, in general, is smaller for foundations with smaller depth. The disagreement may be because, in the model in Bielak (1975), the soil has hysteretic damping and/or because of the difference in the shape of the foundations. 3D prismatic foundations seem to be stiffer, and to have larger radiation damping coefficients, compared to oval foundations, because of the larger contact area with the soil. As it was mentioned in the previous section of this report, the system damping ratio is larger when the radiation damping coefficients are larger, but is smaller

when the foundation is stiffer. In the 3D model in Bielak (1975), it appears that the first factor prevails, while, in the 2D model, the second factor prevails in most of the cases.

The aim of the present study has been to help understand and explain the influence of the various system parameters on the system damping and on the system frequency, for a very simple two-dimensional model. One should bare in mind that the real world is much more complicated than this model. The soil under the building is not a homogeneous halfspace, it may be nonlinear, it also has material damping and only for small relative displacements the vertical base displacement can be decoupled from the base rocking response and the linear analysis holds.

CHAPTER IV

SUMMARY AND CONCLUSIONS

The two-dimensional analytical model of Todorovska and Trifunac (1990) has been employed to measure the damping in the steady-state response of a building during soil-structure interaction, excited by plane SV-waves with oblique incidence. The building has been modeled by a single degree-of-freedom system with rocking stiffness and with a viscous damper, placed on a circular foundation embedded into an elastic homogeneous half-space. The analysis is linear, and the coupling of the vertical motions of the foundation with its horizontal and rocking motions have been neglected.

The system damping of the building-soil model has been measured from the transfer function between the relative building response and the amplitude of the incident wave, using the analogy with the half-power method for a viciously damped single degree-of-freedom system. Both the dynamic and the kinematic interaction have been considered.

The effects of the following factors on the equivalent damping were studied: the height of the building relative to the width of its base, the mass of the building relative to the mass of the foundation and the mass of the replaced soil, the damping in the building, the relative stiffness of the building compared with the soil, the depth of the embedment, and the type of incident waves and their angle of incidence. Incident plane P- and SV-waves were considered.

The conclusions of the study are the following:

1. In the limit when the stiffness of the soil is infinitely large compared with the stiffness of the building, the relative building response approaches the relative response of a fixed-base model. Then the system damping approaches the damping in the building, the system frequency approaches the fixed-base natural frequency, the base rotation goes to zero and the base horizontal motion approaches the horizontal component of the free-field displacements on the surface. When the soil is stiffer, the amplitude of the peak relative response does not depend much on the depth of the embedment, on the type of incident waves and angle of incidence, and the ratio m_b/m_s. It depends only on the damping in the building and on its height.

2. In the limit when the building is very stiff compared with the soil, the system damping and the system frequency asymptotically approach the system damping ς^{rig} and the system frequency η^{rig} of a rigid building welded to the foundation and moving as a rigid body. The relative building response is, then, very small. ς^{rig} is smaller and η^{rig} is lower when the building mass is larger. When the foundation is deeper, ς^{rig} is lower. ς^{rig} is higher when the rotation of the foundation input motion is a significant part of the building excitation (when φH and Δ of the foundation input motion are comparable). η^{rig} does not depend on the type of incident waves and angle of incidence. ς^{rig} does not depend on the damping in the building, ς, and it may happen that it is lower than ς.

3. When both the building and the soil are flexible, the following holds. When the soil is stiffer, the system damping depends more on the building damping, and little on the building mass and height. As the flexibility of the soil increases the effect of the building damping decreases. When the soil is stiffer, in general, the system damping increases as the soil becomes softer. It is higher when the building mass is larger. The system frequency is always lower than the fixed-base natural frequency of the building. The reduction of the system frequency increases as the flexibility of the soil increases and as the mass of the building becomes larger. The relative building response decreases as the flexibility of the soil increases and the mass of the building increases. Under the same conditions the base rotation increases. Both the relative building response and the base rotation decrease as the building damping increases. For flexibility of the soil grater than some critical value (for η_N large enough) the building starts behaving as a rigid body. Then, the system damping decreases with increasing mass of the building and with increasing flexibility of the soil. At the same time the relative building response still decreases. The value of η_N for which this happens is smaller when the damping ratio in the building is higher. In this range, its value is not a measure of the reduction of the building relative response.

4. The relative building response strongly depends on the angle of their incident waves, as do the amplitudes of the free-field motion and consequently, the foundation input motion. The system response is not a function only of the horizontal component of the base input motion, but also depends on the input base rotation, which, in turns, depends on the type of incident waves and angle of incidence. The foundation input motion was found to be more representative as excitation for the building base than the free-field motion. This motion can have a rotational component even when the free-field motion does not ($\gamma = 0°$, $30°$). It was found that the system damping does not depend on the incident angle when the soil is stiffer. When it is softer, the damping is larger for incident SV-waves with incidence beyond critical angle. For the rest of the considered cases, the system damping practically did not depend on the type of incident waves and incident angle.

5. The depth of the embedment may significantly affect the system response. Deeper foundations act "stiffer" and reduce less the system frequency and the relative building response. For the 2D model studied, except for very heavy and tall buildings, the system damping ratio is larger, when the depth of the embedment is smaller. Also, the relative building response is reduced more when the foundation depth is smaller, meaning that then the effective damping in the system response is larger. The opposite has been concluded for embedded 3D prismatic foundations (Bielak, 1975) in previous studies. For smaller η_N, when the soil is stiffer, the peak rocking amplitudes of the base are larger when the embedment depth is smaller. However, for higher η_N, when the building relative response is small and the system behaves similarly to a rigid body embedded into the half-space, the rocking amplitudes are smaller, when the embedment depth is smaller.

REFERENCES

1. Apsel, R.J. and J.E. Luco (1976). "Torsional response of rigid imbedded foundations," J. Eng. Mech. Div., Am. Soc. Civil Engs., **102**(EM6), 957-970.
2. Bielak, J. (1971). "Dynamics of Building-Soil Interaction," Ph.D. Thesis, California Institute of Technology, Pasadena, California.
3. Bielak, J. (1975). "Dynamic Behavior of Structures with Embedded Foundations," Earthquake Eng. Struct. Dyn., **3**, 259-274.
4. Bielak, J. (1976). "Modal analysis for building-soil interaction," J. Eng. Mech. Div., Am. Soc. Civil Engs., **102**(EM5), 771-786.
5. Day, S.M. and G.A. Frazier (1979). "Seismic Response of Hemispherical Foundation," J. Eng. Mech. Div., Am. Soc. Civil Engs., **105**(EM1), 29-41.
6. Lee, V.W. (1979). "Investigation of Three-dimensional Soil-Structure Interaction," Report No. 79-11, Department of Civil Engineering, University of Southern California, Los Angeles, California.
7. Luco, J.E. (1969). "Dynamic interaction of a shear wall with the soil," J. Eng. Mech. Div., Am. Soc. Civil Engs, **95**, 333-346.
8. Luco, J.E. and R.A. Westmann (1971). "Dynamic Response of Circular Footings," J. of Eng. Mech. Div., Am. Soc. Civil Engs, **97**(EM5), 1381-1395.
9. Luco, J.E. (1980). "Soil-Structure Interaction and Identification of Structural Models," Proceedings of 2nd ASCE Conf. on Civil Engineering and Nuclear Power, (Knoxville, Tennessee, Sept. 15-17, 1980), Vol. II, Geotechnical Topics, ASCE, New York, New York, 10.1 - 10.30.
10. Luco, J.E. and R.A. Westmann (1971). "Dynamic Response of Circular Footings," J. of Eng. Mech. Div., Am. Soc. Civil Engs, **97**(EM5), 1381-1395.
11. Rainer, J.H. (1975). "Damping in Dynamic Structure-Foundation Interaction," Can. Geotech. J., **12**, 13-22.
12. Todorovska, M.I. and M.D. Trifunac (1990). "Analytical Model for Building-Foundation-Soil Interaction," Report No. CE 90-01, Department of Civil Engineering, University of Southern California, Los Angeles, California.
13. Trifunac, M.D. (1972). "Interaction of a Shear Wall with the Soil for Incident Plane SH Waves," Bull. Seism. Soc. Amer., **62**(1), 63-83.
14. Trifunac, M.D. and H.L. Wong (1974). "Interaction of a Shear Wall with the Soil for Incident Plane SH Waves: Elliptical Rigid Foundation," Bull. Seism. Soc. Amer., **64**(6), 1825-1842.
15. Tsai, N.-C. (1974). "Modal Damping for Soil-Structure Interaction," J. of Eng. Mech. Div., Am. Soc. Civil Engs, **100**(EM2), 323-341.

LIST OF FREQUENTLY USED SYMBOLS

β, μ, ν	= shear wave velocity, shear modulus, and Poisson's ratio for the soil
h, a	= depth and half-width of the foundation
ω, T	= circular frequency and period of the incident wave
γ	= incident angle (angle between the direction of propagation of the incident wave and the normal to the half-space surface)
$\eta = \frac{\omega a}{\pi\beta} = \frac{2a}{\beta T}$	= dimensionless frequency
H_{sb}, W_{sb}	= height and width of a shear-beam building model
H, r_b	= height and radius of gyration of the equivalent SDOF building model
K_b, C_b	= rotational stiffness and viscous damping of the equivalent SDOF building model
ς, ω_N	= damping ratio and fixed-base natural frequency of the equivalent SDOF building model
m_b, m_f, m_s	= mass per unit length in the y-direction of the building, of the foundation and of the soil replaced by the foundation
ρ_b, ρ_s	= mass density of the building and of the soil
$\eta_N = \frac{\omega_N a}{\pi\beta}$	= dimensionless stiffness parameter of the building relative to the soil
g	= acceleration due to gravity
Δ, V, φ	= horizontal and vertical displacements and rocking angle of point O on the foundation
ψ^{rel}, $u_b^{\text{rel}}, v_b^{\text{rel}}$	= relative angle of rocking and relative horizontal and vertical displacements of the equivalent SDOF building model
u^{ff}	= amplitude of the horizontal component of the free-field motion on the surface
η^{sys}, ς^{sys}	= system frequency and system damping ratio
η^{rig}, ς^{rig}	= limits of η^{sys}, ς^{sys} when the stiffness of the building goes to infinity